AD-A140 743

AFWAL-TR-83-3125

PRELIMINARY EVALUATION OF WAVEGUIDE ABSORBERS

Eric E. Ungar
Leonard G. Kurzweil
Bolt Beranek and Newman Inc.
10 Moulton Street
Cambridge, MA   02238

q 5527

January 1984

Final Report for Period May 1983 to January 1984

FLIGHT DYNAMICS LABORATORY
AIR FORCE WRIGHT AERONAUTICAL LABORATORIES
AIR FORCE SYSTEMS COMMAND
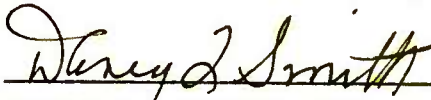WRIGHT-PATTERSON AIR FORCE BASE, OHIO   45433

NOTICE

When Government drawings, specifications, or other data are used for any purpose other than in connection with a definitely related Government procurement operation, the United States Government thereby incurs no responsibility nor any obligation whatsoever; and the fact that the government may have formulated, furnished, or in any way supplied the said drawings, specifications, or other data, is not to be regarded by implication or otherwise as in any manner licensing the holder or any other person or corporation, or conveying any rights or permission to manufacture use, or sell any patented invention that may in any way be related thereto.

This report has been reviewed by the Office of Public Affairs (ASD/PA) and is releasable to the National Technical Information Service (NTIS). At NTIS, it will be available to the general public, including foreign nations.

This technical report has been reviewed and is approved for publication.

VINCENT R. MILLER, Project Engr.
Acoustics & Sonic Fatigue Gp.
Structural Integrity Branch
Structures & Dynamics Division

DAVEY L. SMITH, Chief
Structural Integrity Branch
Structures & Dynamics Div.

FOR THE COMMANDER

RALPH L. KUSTER, Jr., Col., USAF
Chief, Structures & Dynamics Division

"If your address has changed, if you wish to be removed from our mailing list, or if the addressee is no longer employed by your organization please notify AFWAL/FIBED, W-PAFB, OH 45433 to help us maintain a current mailing list."

Copies of this report should not be returned unless return is required by security considerations, contractual obligations, or notice on a specific document.

REPORT DOCUMENTATION PAGE		READ INSTRUCTIONS BEFORE COMPLETING FORM
1. REPORT NUMBER AFWAL-TR-83-3125	2. GOVT ACCESSION NO.	3. RECIPIENT'S CATALOG NUMBER
4. TITLE (and Subtitle) Preliminary Evaluation of Waveguide Vibration Absorbers		5. TYPE OF REPORT & PERIOD COVERED Final Report May 1983 to January 1984
		6. PERFORMING ORG. REPORT NUMBER 5527
7. AUTHOR(s) Eric E. Ungar Leonard G. Kurzweil		8. CONTRACT OR GRANT NUMBER(s) F33615-83-C-3217
9. PERFORMING ORGANIZATION NAME AND ADDRESS Bolt Beranek and Newman Inc. 10 Moulton Street Cambridge, MA 02238		10. PROGRAM ELEMENT, PROJECT, TASK AREA & WORK UNIT NUMBERS 24010175
11. CONTROLLING OFFICE NAME AND ADDRESS Flight Dynamics Laboratory (AFWAL/FIBE) Air Force Wright Aeronautical Laboratories, AFSC Wright-Patterson AFB OH 45433		12. REPORT DATE January 1984
		13. NUMBER OF PAGES 61
14. MONITORING AGENCY NAME & ADDRESS(if different from Controlling Office)		15. SECURITY CLASS. (of this report) UNCLASSIFIED
		15a. DECLASSIFICATION/DOWNGRADING SCHEDULE

16. DISTRIBUTION STATEMENT (of this Report)

Approved for public release, distribution unlimited.

17. DISTRIBUTION STATEMENT (of the abstract entered in Block 20, if different from Report)

Approved for public release, distribution unlimited.

18. SUPPLEMENTARY NOTES

19. KEY WORDS (Continue on reverse side if necessary and identify by block number)

Vibration damping
Vibration absorbers
Waveguide absorbers

20. ABSTRACT (Continue on reverse side if necessary and identify by block number)

The loss factor contribution provided to a vibrating structure by an attached energy-absorbing system is analyzed in terms of the mechanical impedances of the structure and attached system. The driving-point impedance of an exponentially tapered semi-infinite beam is derived and is used to determine the parameters that govern the energy-absorption characteristics of flexural waveguide absorbers.

DD $_{1 \text{ JAN } 73}^{\text{FORM}}$ 1473   EDITION OF 1 NOV 65 IS OBSOLETE

Block 20.

Impedances measured on several preliminary candidate absorber configur-
ations are reported, together with the loss factor contributions they
provided for an experimental plate. Although these configurations were
found not to exhibit the desired waveguide behavior, their measured loss
factor contributions were found to be in good agreement with those predicted
from their measured impedances.

It is concluded that flexural waveguide absorbers indeed have the
potential for providing significant damping, but in order to achieve this
effect, they must be impedance-matched to the structure that is to be
damped, and absorber configurations need to be developed that exhibit the
desired waveguide behavior in the frequency range of concern.

TABLE OF CONTENTS

LIST OF FIGURES

1. INTRODUCTION

Aircraft and spacecraft include a multitude of components which may be adversely affected by vibrations. For example, vibrations may cause airframe or engine parts to suffer premature fatigue fracture, images in optical systems to blur, instrumentation to malfunction, and laser weapons to become ineffective. The control of vibrations and their effects therefore is a significant aspect of aerospace system design and development.

Much work has been done on the design of vibration-resistant structures, as well as on techniques for vibration reduction. These techniques include the well-known vibration isolation approach, detuning (i.e., selecting configurations with small vibration responses to the excitation of concern), the more recently developed methods for increasing the vibratory energy dissipation capabilities (structural damping) of components, and local additions of vibration-suppressing masses or dynamic spring-mass systems (absorbers). All of these classical approaches have been studied rather thoroughly, and the limits on their effectivenesses and ranges of applicability are reasonably well known.

However, there has recently been developed the concept of broadband vibration absorbers, which promises to provide simple and practical vibration control means that not only are highly effective over a broad frequency range, but also relatively easy to apply in practical retrofit situations. It is the purpose of the present report to summarize the results of an exploratory investigation of this novel vibration reduction means.

Section 2 presents a brief discussion of the basic principles of dynamic absorbers, both of the conventional and of the broadband (waveguide) type. In Section 3 there is developed a general expression for the structural damping provided by any type of attached dynamic system. Section 4 presents an analysis of a tapered beam, which represents a tractable approximation to flexural waveguide absorbers that appear to be most practical.

1

Section 5 summarizes the results of some corresponding explora-
tory experiments, and Section 6 presents conclusions and
recommendations.

2. BASIC PRINCIPLES OF DYNAMIC ABSORBERS

2.1 Conventional Absorbers

Dynamic vibration absorbers, which often are also called "tuned dampers," have been studied and applied extensively. They are discussed in handbooks (Ref. 1), as well as in classical textbooks (Refs. 2 and 3). Such an absorber in essence consists of a mass that is attached to a primary vibrating system via a spring or similar resilient element. It is well known that the addition of such an absorber to a dynamic system can alter the system's vibration characteristics significantly, particularly at frequencies in the vicinity of the absorber resonance.

Such classical dynamic absorbers essentially are useful only in situations where the system vibrates at a single constant frequency. By "tuning" the absorber to this frequency - that is, by adjusting the absorber mass and spring stiffness so that the absorber's resonance frequency coincides with the disturbing frequency - one may drastically reduce the system motion at the absorber attachment point. This reduction results because at its resonance frequency such an absorber essentially generates at the attachment point an oscillatory force that acts against the motion of the primary system. However, the desirable vibration reduction effect of such a dynamic absorber is confined to a limited frequency band in the vicinity of the absorber's resonance. The addition of damping to the absorber's spring element tends to broaden the frequency band over which the absorber is effective (and also to reduce its maximum effectiveness); nevertheless, at frequencies outside of this band the effect of the added absorber is either detrimental - in that it increases, rather than decreases, vibrations - or it is negligible.

Some limited investigations have been carried out of absorbers with distributed properties - that is, of absorbers consisting of elastic rods, beams, or plates, rather than of "rigid" masses attached to "massless" springs (Refs. 1, 4, 5). Such

3

distributed parameter absorbers exhibit a multitude of resonances and at each resonance act somewhat like a classical mass/spring absorber; they thus can inhibit vibrations of the primary system in a multitude of frequency bands, but they also increase these vibrations in a multitude of bands. Designing such absorbers so that their attenuation bands match the frequencies of concern is difficult and usually impractical.

2.2 Waveguide Absorbers

All of the aforementioned studies indicate that dynamic absorbers which depend on their resonant responses for their effectiveness can be useful only in relatively narrow and well-defined frequency ranges. This conclusion may also be reached from more general considerations of vibrating systems (Ref. 6).

Vibration absorbers that do not depend on their resonant responses, but which essentially extract energy from a vibrating system by waveguide action, have the potential for attenuating vibrations over wide frequency bands. A "waveguide" is simply a structural system - such as a beam, torsion bar, or plate - along which vibrational waves can travel. If one end of a waveguide is attached to the structure whose vibrations are to be controlled, and the other end is provided with a suitable energy dissipation arrangement (as illustrated schematically in Fig. 2), then this arrangement may be expected to extract vibratory energy from the structure of concern, thus reducing its vibrations.

Realization of the waveguide absorber principle may be illustrated in terms of a damped rod, as shown schematically in Fig. 3. One end of this rod is attached to the structure whose vibrations are to be reduced, and there is provided some damping arrangement, such as a coating of viscoelastic material. As the structure vibrates, it causes compressional waves to propagate along the rod; thus, the absorber conducts energy away from the structure. Due to the damping, the amplitude of the waves

4

decreases as they propagate – and if the damping per wavelength is great enough and the rod length encompasses many wavelengths, then waves reflected from the end of the rod return little energy to the attachment point. In this case the rod essentially exhibits no resonances and behaves in effect like an infinitely long rod that conducts energy away from the driving point.

In order to save weight and also enhance the effectiveness of damping treatments, one may consider use of a tapered rod (see Fig. 4) instead of one of uniform cross-section. In such a rod, the narrowing of the cross-section causes the amplitudes of waves to increase as they propagate away from the wider end, thus improving the dissipation of energy by the damping arrangement. It should be noted that the tapered structural components as waveguides, which have been studied previously (e.g., Ref. 7) and are further investigated in the present report, only facilitate the practical realization of waveguide absorbers, but that wave-guide absorbers in principle need not be tapered.

3. DAMPING CONTRIBUTION FROM ATTACHED SYSTEMS

3.1 Energy Transfer

The impedance Z_A of a system that is to be attached to a vibrating structure at a given point is defined as the ratio of the phasor F of the force acting on the system to the phasor V of the resulting velocity at the driving point

$$Z_A = R_A + jJ_A = F/V \quad . \tag{3-1}$$

The instantaneous power entering the system at the driving point is given by

$$P = Re\{Fe^{j\omega t}\} \cdot Re\{Ve^{j\omega t}\} \quad , \tag{3-2}$$

from which expression one may evaluate the energy D taken on by the system in one cycle, namely

$$D = \int_0^T Pdt \tag{3-3}$$

where the period T obeys

$$T = 2\pi/\omega \tag{3-4}$$

and ω denotes the radian frequency. From the foregoing expressions one finds after a little manipulation that the energy transferred to the system is given by

$$D = \frac{\pi R_A}{\omega} V_0^2 \tag{3-5}$$

where V_0 represents the magnitude $|V|$ of the phasor V.

Consider the structure to which the system is to be attached to be vibrating sinusoidally in time, with a velocity distribution given by $v(x,y)e^{j\omega t}$. Let $V_S = v(x_S, y_S)$ represent the velocity phasor at the attachment point on the structure, and let Z_S denote the impedance of the structure at that point. A force with phasor F acting on the vibrating structure at this point so as to impede its motion then changes the velocity of this point to

$$V = V_S - F/Z_S \quad . \tag{3-6}$$

If this force is due to an attached system, which moves with the same velocity V as the structure and which has an impedance Z_A, then

$$F = Z_A V \quad . \tag{3-7}$$

By combining Eqs. 3-6 and 3-7 one finds that both the attached system and the structural attachment point vibrate with the velocity

$$V = \frac{V_S}{1+Z_A/Z_S} \quad . \tag{3-8}$$

In view of Eq. 3-5, the energy that the attached system extracts from the structure (per cycle) is found to obey

$$D = \frac{\pi R_A}{\omega} \frac{|V_S|^2}{|1+Z_A/Z_S|^2} \tag{3-9}$$

where R_A denotes the real part of the impedance Z_A of the attached system, as implied by Eq. 3-1.

3.2 Contribution to Structural Loss Factor

The loss factor η of a structure is defined in terms of the energy loss per cycle D and the energy W of vibration as

7

$$\eta = \frac{D}{2\pi W} \qquad . \tag{3-10}$$

This energy of vibration is defined as the sum of the total kinetic and potential energies in the structure at any instant. In the steady state, where no net energy is added to the structure or removed from it, the energy of vibration is constant and equal to the kinetic energy at the instant the kinetic energy is at its maximum (and the potential energy is zero). If the structure vibrates in a single mode, all points on the structure move in phase, reaching their velocity (and displacement) maxima simultaneously. For this case, then,

$$W = \frac{1}{2} \int \mu v_0^2 \; dxdy = \frac{1}{2} M_s \overline{v}_0^2 \tag{3-11}$$

where $\mu = \mu(x,y)$ denotes the mass distribution per unit area and $v_0 = v_0(x,y)$ represents the magnitude of $v(x,y)$. The integration extends over the entire structure, and $\overline{v}_0^2$ denotes the mass-weighted spatial average of $v_0^2(x,y)$,

$$\overline{v}_0^2 = \frac{\int \mu v_0^2 dxdy}{\int \mu \, dxdy} = \frac{\int \mu v_0^2 dxdy}{M_s} \tag{3-12}$$

and M_s represents the total mass of the structure. Thus, the loss factor contribution η_A provided to the structure by the attached system is given by

$$\eta_A = \frac{R_A}{\omega M_s} \; \frac{|V_s|^2 / \overline{v}_0^2}{|1 + Z_A / Z_s|^2} \qquad . \tag{3-13}$$

It is evident from the above that the loss factor contribution made by an attached system depends on the original velocity V_s at the attachment point. If this point is a node for which

$V_S = 0$, then clearly $\eta_A = 0$. If the attachment point is an anti-node, on the other hand, then $|V_s|^2/\overline{v_0^2}$ may be relatively large. For example, for beam-like structures with uniformly distributed mass $|V_s|^2/\overline{v_0^2} \approx 2$ in this case, and for plate-like structures with uniformly distributed mass, $|V_s|^2/\overline{v_0^2} \approx 4$. However, for a random attachment point one finds that on the average $|V_s|^2/\overline{v_0^2} = 1$, again for systems with uniformly distributed mass.

Equation 3-13 also indicates that the relation of the attached system's impedance Z_A to the impedance Z_S of the structure at the attachment point has a significant effect on the loss factor contribution η_A. By appropriate differentiation procedures one finds that η_A takes on the greatest value if the well-known impedance-matching condition is satisfied - that is, if Z_A is equal to the complex conjugate of Z_S. For this situation

$$(\eta_A)_{max} = \frac{1}{\omega M_s} \frac{|Z_s|^2}{4R_s} \frac{|V_s|^2}{\overline{v_0^2}} \qquad (3-14)$$

where R_S denotes the real part of the structure's impedance at the attachment point (and here is equal to R_A).

It should be noted at a structural resonance, the imaginary part of the structural impedance vanishes, so that $Z_S = R_S$, and the maximum loss factor contribution for this case becomes

$$(\eta_A)_{\substack{max \\ res}} = \frac{R_s}{4\omega M_s} \frac{|V_s|^2}{\overline{v_0^2}} \quad . \qquad (3-15)$$

9

4. ANALYSIS OF TAPERED BEAM ABSORBERS

4.1 Motivations for Analysis

In Section 2, the idea of waveguide absorbers was illustrated in terms of uniform or tapered rods (Figs. 3 and 4) that propagate compressional (longitudinal) waves along their length. Although such longitudinal waveguides are relatively easy to visualize and analyze, they are of limited practical interest. The comparatively high wavespeeds associated with compressional waves in commonly available materials restrict the utility of absorbers consisting of compressional waveguides to frequency regions that are higher than those usually of concern.

The speeds of flexural waves typically are much lower than those of compressional waves. Flexural waveguide absorbers therefore may be expected to be effective in the frequency domains of interest for structural and mechanical system applications. In fact, the waveguide absorbers that have been built and tested for practical applications (Refs. 7, 8) rely either entirely or predominantly on flexural wave action.

A flexural waveguide absorber may be visualized readily in terms of a beam attached to the vibrating system from which energy is to be extracted. Figure 5 is a schematic sketch indicating how a double-cantilever may be attached to such a system via a rigid stand-off connection.

As is the case for waveguide absorbers that rely on compressional waves, flexural waveguide absorbers need not be tapered to function, but tapered flexural absorbers may be expected to be lighter and to be damped more effectively by a given treatment than similar absorbers with uniform cross-sections. The analysis presented in the present section was undertaken therefore to provide an understanding of the parameters that affect the performance of tapered flexural waveguide absorbers.

10

4.2 Impedance of Tapered Beam

General sinusoidal flexure

The equation of lateral motion of a slender beam, in absence of rotatory inertia and transverse shear effects, may be written (Ref. 9) as

$$\frac{\partial}{\partial x^2}\left[EI\,\frac{\partial^2 u}{\partial x^2}\right] + \rho A\,\frac{\partial^2 u}{\partial t^2} = 0 \qquad (4\text{-}1)$$

where u denotes the lateral displacement, x a length-wise coordinate, and t, time. The beam's properties are represented by the elastic modulus E and density ρ of the material, and by the area A of the beam's cross section and its centroidal moment of inertia I. In general, both EI and ρA may be functions of x.

For the case of sinusoidal motion one may introduce complex (phasor) notation and define

$$u = Ue^{-j\omega t} \qquad (4\text{-}2)$$

where U denotes the phasor of u. If E and ρ are constant, so that

$$c = \sqrt{E/\rho} \qquad (4\text{-}3)$$

represents the constant longitudinal wavespeed in the beam material, one may reduce Eq. 4-1 to the following differential equation for U(x):

$$\frac{d^2 I}{dx^2}\cdot\frac{d^2 U}{dx^2} + 2\,\frac{dI}{dx}\,\frac{d^3 U}{dx^3} + I\,\frac{d^4 U}{dx^4} = A\,\frac{\omega^2}{c^2}\,U \qquad . \qquad (4\text{-}4)$$

The solutions for U clearly depend on the I(x) and A(x) functions. Although one may conceive of various beam configurations that are of practical interest, closed-form mathematical solutions can be obtained for only very few. It is instructive to investigate the case that is most easily analyzed - that of a

11

beam of uniform thickness with exponentially varying width, for which one may take

$$I(x) = I_0 e^{-2\beta x} \quad , \qquad A(x) = A_0 e^{-2\beta x} \quad . \qquad (4\text{-}5)$$

Substitution of these relations into Eq. 4-4 permits one to reduce that equation to

$$(2\beta)^2 \frac{d^2 U}{dx^2} - 4\beta \frac{d^3 U}{dx^3} + \frac{d^4 U}{dx^4} = B^2 U \qquad (4\text{-}6)$$

where

$$B = \omega/cr \, , \qquad r = \sqrt{I_0/A_0} \quad . \qquad (4\text{-}7)$$

Note that r represents the radius of gyration of the beam cross-sectional area at $x = 0$.

For assumed solutions of Eq. 4-6 of the form $U = e^{px}$, one finds that p must satisfy

$$p^2 [(2\beta)^2 - 4\beta p + p^2] = B^2 \qquad (4\text{-}8)$$

and thus

$$p = \beta \pm \sqrt{\beta^2 \pm B} \quad . \qquad (4\text{-}9)$$

The general solution of Eq. 4-6 therefore may be written as

$$U(x) = e^{\beta x} \left[C_{++} e^{x\sqrt{\beta^2 + B}} + C_{-+} e^{-x\sqrt{\beta^2 + B}} + C_{+-} e^{x\sqrt{\beta^2 - B}} \right.$$

$$\left. + C_{--} e^{-x\sqrt{\beta^2 - B}} \right] \qquad (4\text{-}10)$$

where the C's are constants that depend on the boundary conditions.

Cutoff frequency for energy propagation

For the case where $B < \beta^2$, all four values of p of Eq. 4-9 are real quantities, and all four terms of Eq. 4-10 correspond to non-propagating components.* In this case no energy propagates along the beam. For $B > \beta^2$, however, one may rewrite Eq. 4-10 as

$$U(x) = e^{\beta x}[C_{++}e^{x\sqrt{B+\beta^2}} + C_{-+}e^{-x\sqrt{B+\beta^2}} + C_{+-}e^{jx\sqrt{B-\beta^2}}$$

$$+ C_{--}e^{-jx\sqrt{B-\beta^2}}] \tag{4-11}$$

where the last two terms correspond to propagating components.

In view of Eq. 4-7, there thus corresponds to $B = \beta^2$ a "cutoff" frequency ω_0, given by

$$\omega_0 = cr\beta^2 \tag{4-12}$$

which marks the dividing line between non-propagating and propagating conditions; energy propagation occurs only for $\omega > \omega_0$.

Driving-point impedance

Consider now a semi-infinite beam extending from $x = 0$ in the positive x direction, with excitation applied at $x = 0$ and acting at a frequency that is above the cutoff frequency. If $U(x)$ is to remain finite, then C_{++} must vanish. Furthermore, the

---

*If α is real and positive, motion described by $u = Ce^{\pm\alpha x}e^{-j\omega t} = Ce^{\pm\alpha x - j\omega t}$ corresponds to all points moving in phase, but with different amplitudes. On the other hand, $u = De^{j(\alpha x - \omega t)}$ corresponds to a wave traveling in the direction of positive x, and $u = De^{j(-\alpha x - \omega t)}$ corresponds to a wave traveling in the direction of negative x. If D is constant, then the motions are everywhere of the same amplitude, but not of the same phase. If D is a function of x, then so is the amplitude (see Ref. 10).

condition that no energy propagates from infinity toward the origin requires that C_{--} vanish. For this case, then, Eq. 4-11 may be rewritten as

$$U(x) = C_{-+}e^{(\beta - \sqrt{B+\beta^2})x} + C_{+-}e^{(\beta + j\sqrt{B-\beta^2})x} \qquad . \quad (4-13)$$

The shear force that acts on the beam is given by

$$Q = \frac{\partial}{\partial x}\left[EI\,\frac{\partial^2 u}{\partial x^2}\right] \qquad\qquad\qquad (4-14)$$

and for a beam with constant E and with cross-sectional properties that vary as given by Eq. 4-5, obeys

$$Q = \left[-2\beta\,\frac{d^2U}{dx^2} + \frac{d^3U}{dx^3}\right] EI_0 e^{-2\beta x}\, e^{-j\omega t} \qquad . \quad (4-15)$$

The impedance of the beam at the origin $x = 0$, in view of the definition of impedance, obeys

$$Z_B = \frac{Q}{\partial u/\partial t}\bigg|_{x=0} \qquad\qquad\qquad (4-16)$$

In view of Eqs. 4-2, 4-15 and 4-16,

$$Z_B = \frac{EI_0[-2\beta U''(0) + U'''(0)]}{-j\omega U(0)} \qquad , \quad (4-17)$$

where the primes indicate differentiation with respect to x. By substitution for U from Eq. 4-13 and requiring the beam to be rotation- free at $x = 0$ (as for a rigidly guided beam or one that is half of a beam part that is symmetric about the origin), - i.e., requiring $U'(0) = 0$, one finds after considerable manipulation that one may rewrite Eq. 4-17 for frequencies above the cutoff frequency as

$$Z_B = R_B + jJ_B = 2m_B\omega_0\,[\phi_R(F) + j\phi_J(F)] \qquad (4-18)$$

14

where

$$\phi_R(F) = \sqrt{F-1} \ [\sqrt{1 + 1/F} + 1/\sqrt{F}]^2 \qquad (4-19)$$

$$\phi_J(F) = 2/F + (1-2/F) \ \sqrt{1+F}$$

$$F = \omega/\omega_0 \quad .$$

and where

$$m_B = \int_0^\infty \rho A_0 \ e^{-2\beta x} \ dx = \rho A_0/2\beta \qquad (4-20)$$

corresponds to the total mass of the semi-infinite beam under discussion.

For high frequencies - that is, for $F \gg 1$ - one finds that $\phi_R \approx \phi_J \approx \sqrt{F}$, so that

$$Z_B \Big|_{F \gg 1} \approx 2m_B \omega_0 \sqrt{\frac{\omega}{\omega_0}} \ (1+j) = \rho A_0 \ \sqrt{c r \omega} \ (1+j) \quad . \qquad (4-21)$$

This is just one half of the impedance of an infinite beam (Ref. 10) with constant cross-section area A_0, in agreement with what one would expect.*

One may also observe that $\phi_R(1) = 0$, implying that $R = 0$ for $\omega = \omega_0$, or that no energy is absorbed by the beam at the cut-off frequency. Again, this agrees with what one would expect, since no energy can propagate along the beam at and below the cutoff frequency.

_____

*The beam analyzed here is semi-infinite and has the same con-
 straint at $x = 0$ as an infinite beam, where zero rotation at the
 origin is enforced by symmetry. Because no energy is reflected
 back to the driving point, only the beam properties at this
 point come into play.

For frequencies below the cutoff frequency, on the other hand, ϕ_R vanishes and one may show that

$$Z_B\Big|_{F \ll 1} = j\omega m_B \quad .\tag{4-22}$$

At these low frequencies, thus, the impedance of the beam is just that of a rigid mass equal to that of the beam - once again as one would expect.

4.3 Loss Factor Contribution of Tapered Beam as Waveguide Absorber

The loss factor contribution η_B that a tapered beam makes to a vibrating system to which it is attached may be calculated by substituting the beam's impedance into Eq. 3-13 in place of the general attached-system impedance. For the semi-infinite tapered beam discussed in the foregoing paragraphs, one thus finds one may use Eqs. 4-18 and 4-19 to write

$$\eta_B = \frac{2m_B}{M_s} \frac{\phi_R}{F_s} \frac{|V_s|^2/\overline{v}_0^2}{\left|1 + \dfrac{2\omega_0 m_B(\phi_R + j\phi_j)}{Z_s}\right|^2} \quad .\tag{4-23}$$

This expression may then be employed to investigate how this loss factor contribution to specific structures varies with the ratio of the absorber mass to the structure mass, with the frequency ratio F and with the other parameters appearing in this expression.

4.4 Rotational Excitation of Tapered Beam

The analyses presented in the foregoing paragraphs were based on the assumption that the tapered beam was excited by a pure force and that its rotation at the driving point was zero.

Although this assumption may constitute a realistic approximation to many practical situations - particularly to those where there exists a single fastening point and where thus the rotational stiffness of the attachment is relatively small - it is of interest to investigate the loss factor contribution resulting from rotational inputs to the tapered beam.

If one notes that the moment M_B and the angular velocity Ω at the origin of a beam are given by

$$M_B = - EI \left. \frac{\partial^2 u}{\partial x^2} \right]_{x=0} \tag{4-24}$$

$$\Omega = \left. \frac{\partial^2 u}{\partial x \partial t} \right]_{x=0} \tag{4-25}$$

then one may evaluate the rotational driving point impedance

$$Z_{\theta B} = M_B / \Omega \tag{4-26}$$

of a tapered beam above its cutoff frequency by substituting Eq. 4-13 into the foregoing expressions and using the boundary condition $U(0) = 0$. The result may be written as

$$Z_{\theta B} = R_{\theta B} + j J_{\theta B}$$

$$= \frac{EI_0}{\beta rc} \left[\frac{\sqrt{F-1}}{F} + j \frac{\sqrt{F+1} - 2}{F} \right] \quad . \tag{4-27}$$

This loss factor contribution due to energy transmitted to an attached absorber by angular motion at the attachment point may be written, in analogy to Eq. 3-13, as

$$\eta_\theta = \frac{R_{\theta B}}{\omega M_s} \frac{|\Omega_s|^2 / \overline{v}_0^2}{\left| 1 + \dfrac{Z_{\theta B}}{Z_{\theta s}} \right|^2} \tag{4-28}$$

17

where $Z_{\theta R}$ denotes the point-moment impedance of the structure to which the absorber beam is attached and $|\Omega_s|$ represents the amplitude of the angular velocity of the structure at the attachment point in absence of the absorber. Both $Z_{\theta s}$ and Ω_s here correspond to the direction related to bending of the attached beam about an axis perpendicular to its length.

In order to compare η_θ to η, one needs to know the relation between $|\Omega_s|$ and $|V_s|$. For plate-like structures, this is complicated; it depends both on the mode shape and on the orientation of the absorber beam. For a structure consisting of a uniform beam whose axis is parallel to that of the absorber beam, this relation is simpler, but still depends on the mode shape and on the specific location of the attachment point. However, one determines that

$$|\Omega_s|^2_a = k^2_s \ |V^2_s|_a \qquad (4\text{-}29)$$

where the added subscript a indicates the spatial average of the quantity. Here k_s denotes the wavenumber of the flexural vibration of the structural beam and obeys

$$k^2_s = \left(\frac{2\pi}{\lambda}\right)^2 = \frac{\omega}{r_s C_{Ls}} \qquad (4\text{-}30)$$

where λ denotes the bending wavelength of the structural beam at frequency ω; r_s represents the radius of gyration of that beam's cross-section, and C_{Ls} denotes the longitudinal wavespeed in the material of that beam.

For the case where $|\Omega_s|$ and $|V_s|$ are related as in Eq. 4-29, one finds that

$$\frac{\eta}{\eta_\theta} = \frac{r_s C_{Ls}}{rc} \frac{|1 + Z_\theta/Z_{s\theta}|^2}{|1 + Z/Z_s|^2} \left[\sqrt{1 + 1/F} - 1/\sqrt{F}\right]^2 \quad . \qquad (4\text{-}31)$$

One may note that the expression involving the frequency ratio F here is equal to $(\sqrt{2} - 1)^2 \approx .17$ for $F = 1$ and increases monotomically toward unity for large F. This implies that the rotational loss factor contribution η_θ here is equal to the translational contribution η for large F, but that $\eta_\theta > \eta$ for small F – provided that the terms of Eq. 4-31 that do not contain F explicitely are equal to unity, something that may occur only in some special cases that are beyond the scope of the present study.

5. EXPLORATORY EXPERIMENTS

5.1 Experimental Absorbers and Plate Structure

A brief experimental study was carried out in order to investigate the applicability of the foregoing theoretical results and to gain insight into the performance of broadband absorbers. A tapered beam (see Fig. 6) was built and its impedance measured in order to provide a check on the theory developed in Section 4.2. In addition, two disks, each with 8 spiral cuts (see Fig. 7) were built. These disks were modeled after similar ones described by the German investigators [7]; they were expected to act like a multi-beam vibration absorber and could be constructed relatively easily. The impedances of the two spiral disks (individually and in combination) were measured. In addition, their effect on the loss factor of an experimental plate was evaluated experimentally in order to assess the validity of the theory developed in Section 3.2.

Each absorber was made of 1/16 in. aluminum plate with 1/8 in. thick damping material (E-A-R ISODAMP C-2003) adhered to the surface. The manufacturer's literature give the following values of the damping material properties at room temperature and in the frequency range 100 - 10,000 Hz:

$$\rho = 1714 \text{ kg/m}^3 \quad (107 \text{ lb/ft}^3)$$

$$E = 2 \times 10^9 \frac{N}{m^2}$$

$$\eta = 0.5 \quad .$$

Figure 8 shows the experimental plate, used as the "struc-
ture" to which the absorbers were attached in order to investi-
gate their effect on the structure's loss factor. The plate was
designed to have no parallel edges, so as to facilitate achieving
a fairly uniform vibration field. Holes where the absorbers
could be bolted to the plate were provided at three positions:
position 1 near the center of the plate, position 2 near an edge,
and position 3 at an in-between location. All of the results
presented here are for the absorber attached at position 3, which
is expected to be the most representative location. Figure 9
shows the three methods used for attaching the absorbers to the
plate; they were selected for their convenience and so as to
provide enough standoff to permit the absorbers to vibrate
freely.

5.2 Impedances

Figure 10 shows the instrumentation system used for measur-
ing the mechanical impedance of the absorbers and the plate. The
test specimen was subjected to broadband excitation via an impe-
dance head attached to an electrodynamic shaker.

An HP 5423A Dual Channel Analyzer was used to obtain the
real and imaginary parts of the impedance from the simultaneous
force and acceleration signals generated by the impedance head.

Figure 11 shows the experimentally determined real and imag-
inary parts of the input impedance at the center of the tapered
beam (including the mass of the studs, nuts and washers, shown in
Fig. 9 as used to attach the single absorbers to the plate). The
measured real and imaginary parts of the impedance of this
attachment hardware alone are shown in Fig. 12. As expected, the
impedance of the attachment hardware is essentially that of a
mass; i.e. the attachment hardware responds as a rigid body with
an impedance $Z_{attachment} \approx j\omega M_{att}$, where M_{att} = 48 gms

21

is the mass of the attachment hardware plus the impedance head mass in front of the force gage of the impedance head.

The impedance of the tapered beam alone (without attachment hardware) was obtained by subtracting the real and imaginary parts of $Z_{attachment}$ (Fig. 12) from the real and imaginary parts of $Z_{beam + attachment}$ (Fig. 11). The results are shown in Fig. 13.

Also shown in this figure as dashed lines are the theoretical real and imaginary parts of the impedance of a centrally-driven infinitely long tapered beam (symmetrical about the driving point at x = 0, with the beam tapered in both the +x and -x directions). The theoretical impedance values shown are twice those for a one-sided semi-infinite beam, given by Eq. 4-18; $R_0 = 19.0$ kg/s and $f_0 = 2\pi\omega_0 = 29.0$ Hz.

It is clear from this figure that the impedance of the experimental tapered beam does not exhibit the theoretical infinitely-long beam behavior. Even at the high frequencies where the impedance no longer exhibits the effects of individual resonants, the real part of the impedance does not appear to be approaching the theoretical solution. A possible explanation is that the center portion of the experimental beam, which is not covered by damping material (see Fig. 6), deforms like a spring and isolates the mass of the beam to some extent.

Figures 14 and 15 show the measured impedances of a centrally-driven 8-spiral disk (see Fig. 7) with and without attachment hardware. Figure 16 show the measured impedance of two 8-spiral disks, arranged as shown in Fig. 10b.

The results of measurements of the plate impedance are shown in Fig. 17. The coherence between the force and acceleration signals was poor at frequencies below about 3000 Hz, so that these measured impedances are inadequate. For subsequent calcu-

lation purposes, the theoretical impedance for an infinite plate (shown as dashed lines in Fig. 17) was used.

5.3 Loss Factors

The experimental set-up used for measuring the loss factor of the plate, with and without the absorbers attached, is shown in Fig. 18. The plate was excited in 1/3 octave bands by the sound pressure from an acoustic driver placed close to the plate. The excitation was switched off and the time history of the 1/3 octave band acceleration level (in dB) of the plate was obtained using a Graphic Level Recorder. The reverberation time T_{60}* for each 1/3 octave band was determined from the slope of the acceleration level time history curve (see for example, Fig. 20). The loss factor was then computed from (Ref. 10)

$$\eta = \frac{2.2}{T_{60}f} \tag{5-1}$$

where f is the 1/3 octave band center frequency.

Figures 20-22 present the measured loss factors of the plate with an 8-spiral disk bolted to it, an 8-spiral disk expoxied to it, and two 8-spiral disks bolted to it, all at position 3. Also shown on these figures are the measured loss factors for the undamped plate (η_P), as well as the calculated loss factors.

The calculated loss factor of the plate with the attached absorber was obtained by adding to the measured loss factor η_P of the plate without the absorber the calculated plate loss factor contribution η_A made by the absorber. The latter was calculated from Eq. 3-13, using for $Z_A = R_A + jJ_A$ the measured driving-point (force) impedances of the absorbers and the attachment hardware,

---

*T_{60} is the time in seconds required for the acceleration level to decay by 60 dB.

assuming $|V_s|^2/\overline{v_0^2} = 1$, and using for Z_S the theoretical impedance
of an infinite plate;* that is

$$Z_S = Z_P \approx 2.3 \ c_L \rho h^2/(1-\nu^2) \tag{5-2}$$

where h denotes the plate's thickness, ρ the density, c_L the
longitudinal wave speed and ν the Poisson's ratio of the plate
material. For the experimental plate, $Z_S = 165$ kg/s and $M_S =$
6.37 kg.

5.4 Discussion of Results

Figures 20-22 indicate that the addition of the absorbers
typically increased the plate loss factor by a factor of about 2.
The theoretically obtained loss factors shown in these figures
are of the same order of magnitude as the measured ones, although
they appear to be too high at frequencies below about 600 Hz.

The reasons for this are not clear. Possible explanations
include errors in the measured impedances of the absorbers, the
assumption that the experimental plate impedance can be modeled
as that of an infinite plate, and inaccuracies in the measurement
of the plate loss factors. Since the measured impedance of the
two 8-spiral disks in combination agrees well with the sum of the
impedances of the individual 8-spiral disks measured individu-
ally, it is probable that the experimentally determined absorber

---

*From Ref. 10 one may calculate that a one-third octave band
 centered at 125 Hz contains 5.5 modes of the experimental plate,
 and that the number of modes in other one-third octave bands is
 proportional to the band's center frequency. Thus, many plate
 modes typically occur in any given one-third octave band in the
 measurement range. This fact implies that the spatial average
 condition $|V_s|^2/v_0^2 = 1$ should be a reasonable one to apply and
 also that the infinite plate impedance should be a good approxi-
 mation in the frequency-average (Ref. 6).

impedances are correct. Also, since the number of resonant modes in each 1/3 octave band for the experimental plate is high (see footnote accompanying Eq. 5-2), the infinite plate impedance should be a good approximation to the frequency-average of the impedance in each 1/3 octave band considered here. Thus, inaccuracies in the measured loss factors appear to be the most likely source of the discrepancies between theory and experiment.

It is instructive to compare the loss factor contributions of the experimental spiral disk absorbers with the comparable maximum loss factor contributions that can be obtained - i.e., those obtained by means of an absorber that is impedance-matched to the plate. For this purpose, values of $\eta_A/(|v_p|^2/\overline{v}_0^2)$ calculated from Eq. 3-13 for the experimental absorbers (using the measured values of Z_A and the theoretical value of Z_S) are shown in Fig. 23 together with the maximum values calculated from Eq. 3-14. One may note that in the high frequency range (above about 2000 Hz) the absorber with the least attachment hardware (i.e., the one epoxied to the plate) gives the best performance (nearly optimum). For this absorber configuration, the imaginary part of the impedance is very close to zero, thus approximately satisfying that part of the impedance matching condition for maximizing η_A that requires the imaginary part of Z_A to be the negative of that of Z_S (since the plate impedance Z_S is purely real). For the other two absorbers (with more attachment hardware mass) the imaginary parts of Z_A at high frequencies are larger, resulting in poorer impedance matching.

Figure 24 presents a comparison of the loss factor increases achievable for the experimental plate with three idealized damping treatments of the same weight - i.e., 168 gm or about 2.6% of the plate weight. These treatments consist of:

a) An 8-spiral disk absorber, ideally impedance-matched to the plate, attached to it so that $|V_s|^2/\overline{v}_0^2 = 1$ (see footnote accompanying Eq. 5-2) and without taking advan-

tage of additional damping potentially available from
rotational excitation of the absorber.

b)   A thin, rigidly attached single layer of a highly effec-
tive viscoelastic material with assumed frequency-
independent loss modulus (E-A-R ISODAMP C-2003; see p.
20 for property values).

c)   An optimized constrained layer treatment consisting of
an aluminum cover plate of about 2 mils thickness
attached to the basic plate via an extremely thin layer
of an ideal viscoelastic material with frequency-
independent loss factor of 0.5 and low shear modulus,
designed for optimum performance at 1 kHz.

Also shown in the figure is a curve corresponding to the best
practically feasible constrained layer treatment, as discussed
later.

The loss factors of the theoretical viscoelastic layer
treatments were calculated using relations from Ref. 11 and are
based on the assumption that the viscoelastic materials can be
obtained in suitable thicknesses and can be attached to the
plate(s) by means of extremely thin adhesive layers.   In fact, a
free viscoelastic layer would need to be about 3 mils thick, and
the aluminum cover plate atop a constrained viscoelastic layer
would need to be about 2 mils thick for the treatments to weigh
the same as a single waveguide absorber.   These thicknesses are
marginally practical.

The frequency at which the greatest loss factor of a plate
with a constrained layer treatment occurs varies very nearly
inversely with the thickness of the viscoelastic material and
directly as the material's shear modulus.   By selecting different
viscoelastic layer thicknesses one can thus in effect shift the
corresponding loss factor curve parallel to the frequency axis.
Extremely thin constrained viscoelastic layers of practical

26

materials thus correspond to damping peaks at very high frequencies and tend to result in very low loss factors at the frequencies of interest. The theoretical curve indicated in Fig. 24 corresponds to a 0.1 mil thick viscoelastic material with a shear modulus of the order of 10 psi; a lower modulus and/or greater viscoelastic material thickness would be required to shift the damping peak to lower frequencies.

The foregoing constrained layer parameters are clearly impractical. If one assumes a 1.8 mil covering layer constraining a 0.5 mil layer of a viscoelastic material with the lowest practically likely shear modulus of 1000 psi one obtains what is probably the best practically achievable configuration. Its performance, as evident from the figure, is considerably poorer than that of the ideal configuration.

It appears from Fig. 24 that for a uniform thin plate like the one investigated experimentally, optimized constrained or free viscoelastic layer treatments can in theory provide greater damping than an optimum waveguide absorber of the same weight, except perhaps at low frequencies. However, a waveguide absorber here may be expected in practice to outperform a constrained layer treatment over most of the frequency range of concern, as well as having constructional advantages (e.g., ease of manufacture, attachment, dimensional control) over both types of viscoelastic layer treatments.

6. CONCLUDING REMARKS

6.1 Summary

Expressions have been developed that indicate the loss factor contributions which idealized tapered beam absorbers can make to vibrating systems to which they are attached. Although one can conceive of other types of absorber configurations, tapered beams may be considered representative of absorbers that work on the basis of flexural motions of damped systems.

The analytical expressions, which may be used for design guidance, display the important parameter dependences. As also is evident from experimental results, these expressions indicate the importance of matching the absorber's impedance to that of the structure to which it is to be attached; mismatching tends to reduce an absorber's effectiveness severely.

It is also evident from the analytical results for a tapered beam attached to a structure that for the case where the structure's impedance is much greater than the attached absorber's impedance, the loss factor contribution made by the absorber is proportional to the ratio of the absorber mass to the structure mass.

The sample absorbers used for the exploratory plate damping experiments reported here were constructed ad hoc, essentially copying similar absorbers described in the literature, without any effort at development. The measured mechanical impedance data show that these sample absorbers generally do not exhibit the desired waveguide behavior and also do not perform like the absorbers for which data appears in the literature. It appears that more careful design and development are required to obtain waveguide absorbers with improved practical performance.

Although the results obtained in this too brief preliminary study are incomplete and far from fully conclusive, it appears that appropriately developed and well-selected waveguide absorb-

ers are promising means for providing significant amounts of structural damping. They may be expected to be particularly useful for relatively massive structures and at relatively low frequencies, for which viscoelastic coatings and laminates tend to be ineffective, or for other configurations, such as thin-walled structures, where viscoelastic treatments may be too heavy or otherwise impractical. They may be especially attractive for vibration control applications in retrofit situations.

6.2 Recommendations

In view of the promising results that have been described in the literature and the preliminary nature of the results of the exploratory investigation summarized here, it appears that wave-guide absorbers merit further study.

Development efforts appear advisable that address (a) better consideration of rotational inputs, to take advantage of this additional path for extracting energy from a vibrating structure, (b) improved attachment details to ensure the transfer of energy into energy-dissipating motions of the absorbers, and (c) absorber configurations with higher modal densities and greater built-in damping, to obtain better waveguide action at lower frequencies.

It would also be of value to carry out comparison studies of waveguide absorbers and more conventional damping means, particu-larly for relatively large and massive structures, for which wave-guide absorbers may be expected to be particularly advantageous.

REFERENCES

1. F.E. Reed, "Dynamic Vibration Absorbers and Auxiliary Mass Dampers." Chapter 6 of <u>Shock and Vibration Handbook</u>, 2nd Edition, Ed. by C.M. Harris and C.E. Crede. McGraw-Hill Book Co., Inc., New York, 1976.

2. J.P. Den Hartog, <u>Mechanical Vibrations</u>, McGraw-Hill Book Co., Inc., New York, 4th Edition, 1956.

3. J.C. Snowdon, <u>Vibration and Shock in Damped Mechanical Systems</u>, John Wiley & Sons, Inc., New York, 1968.

4. J.C. Snowdon, "Platelike Dynamic Vibration Absorbers," <u>J. Engineering for Industry</u> (Trans. ASME), Feb. 1975, pp. 88-93.

5. M.A. Nobile and J.C. Snowdon, "Viscously Damped Absorbers of Novel Design," <u>J. Acous. Soc. Am.</u>, **61**, 5 (May 1977), pp. 1198-1208.

6. E. Skudrzyk, <u>Simple and Complex Vibratory Systems</u>, The Pennsylvania State University Press, University Park, PA, 1968.

7. O. Bschorr and H. Albrecht, "Schwingungsabsorber zur Reduzierung des Maschinenlaerms" (Vibration absorbers for the reduction of machinery noise), <u>VDI-Zeitschrift</u>, **121** (1979), pp. 253-261.

8. P.J. Van den Brulle, "Entwicklung von Schwingungsabsorber zur Herabsetzung von Vibrations-belastung" (Development of Vibration Absorbers for the Reduction of Vibratory Loading," Messerschmitt-Boelkow-Blohm Report No. MBB/FE 17/ZTL/R/12 (31 Jan. 1980).

9. R.P. Goel, "Transverse Vibrations of Tapered Beams," <u>J. Sound and Vib.</u>, **47** (1), pp. 1-7, 1976.

10. L. Cremer, M. Heckl, E.E. Ungar, <u>Structure-Borne Sound</u>, Springer-Verlag, New York, 1973.

11. E.E. Ungar, "Damping of Panels." Chapter 14 of <u>Noise and Vibration Control</u>, Ed. by L.L. Beranek. McGraw-Hill Book Co., New York, 1971.
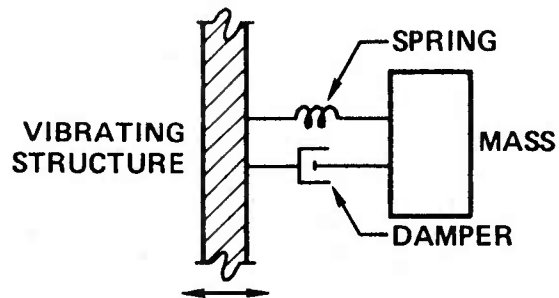
FIG. 1.   SCHEMATIC DIAGRAM OF CLASSICAL DYNAMIC ABSORBER.
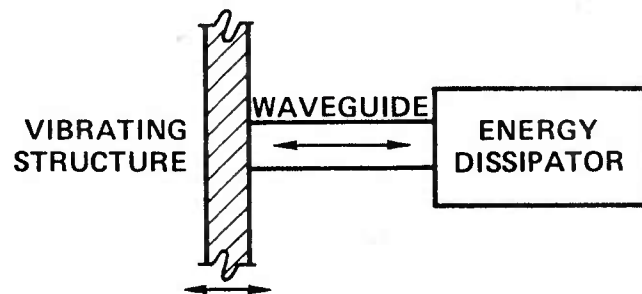
FIG. 2.   SCHEMATIC DIAGRAM OF WAVEGUIDE ABSORBER ACTION
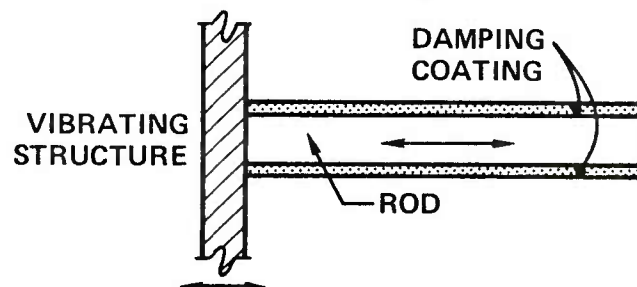
FIG. 3.   SCHEMATIC SKETCH OF WAVEGUIDE ABSORBER CONSISTING OF
DAMPED ROD CARRYING LONGITUDINAL WAVES.
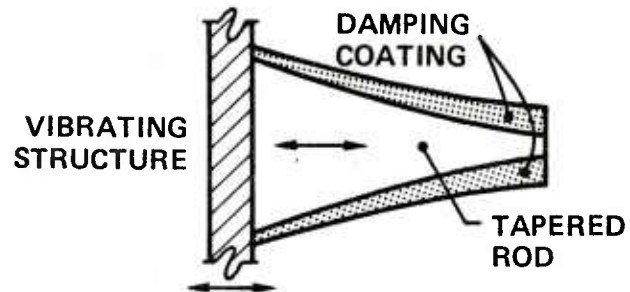
FIG. 4. SCHEMATIC SKETCH OF LONGITUDINAL WAVEGUIDE ABSORBER
CONSISTING OF TAPERED DAMPED ROD.
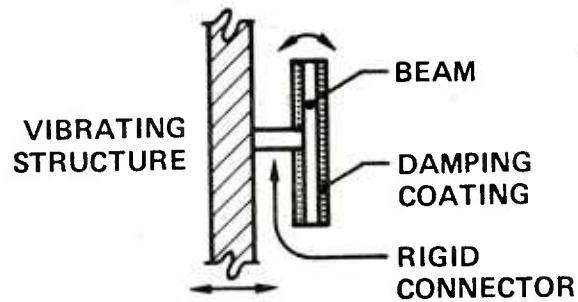
FIG. 5. SCHEMATIC SKETCH OF FLEXURAL WAVEGUIDE ABSORBER CONSIST-
ING OF DAMPED BEAM.
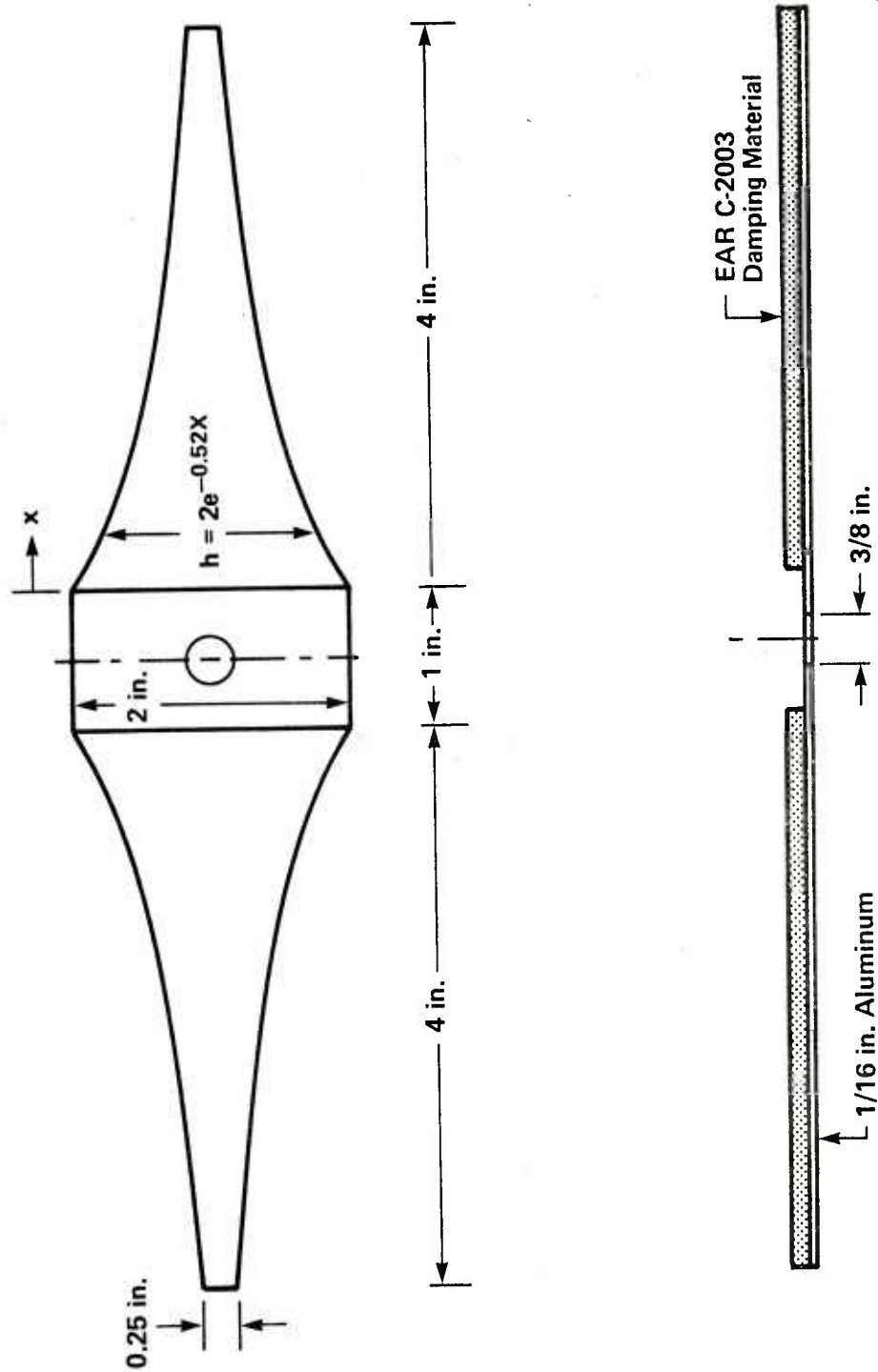
FIG. 6. DIMENSIONS OF TAPERED EXPERIMENTAL BEAM.

33

6 3/8"

ALUM. PLATE (1/16" THICK)

HOLE FOR 3/8" STUD

DAMPING MATERIAL
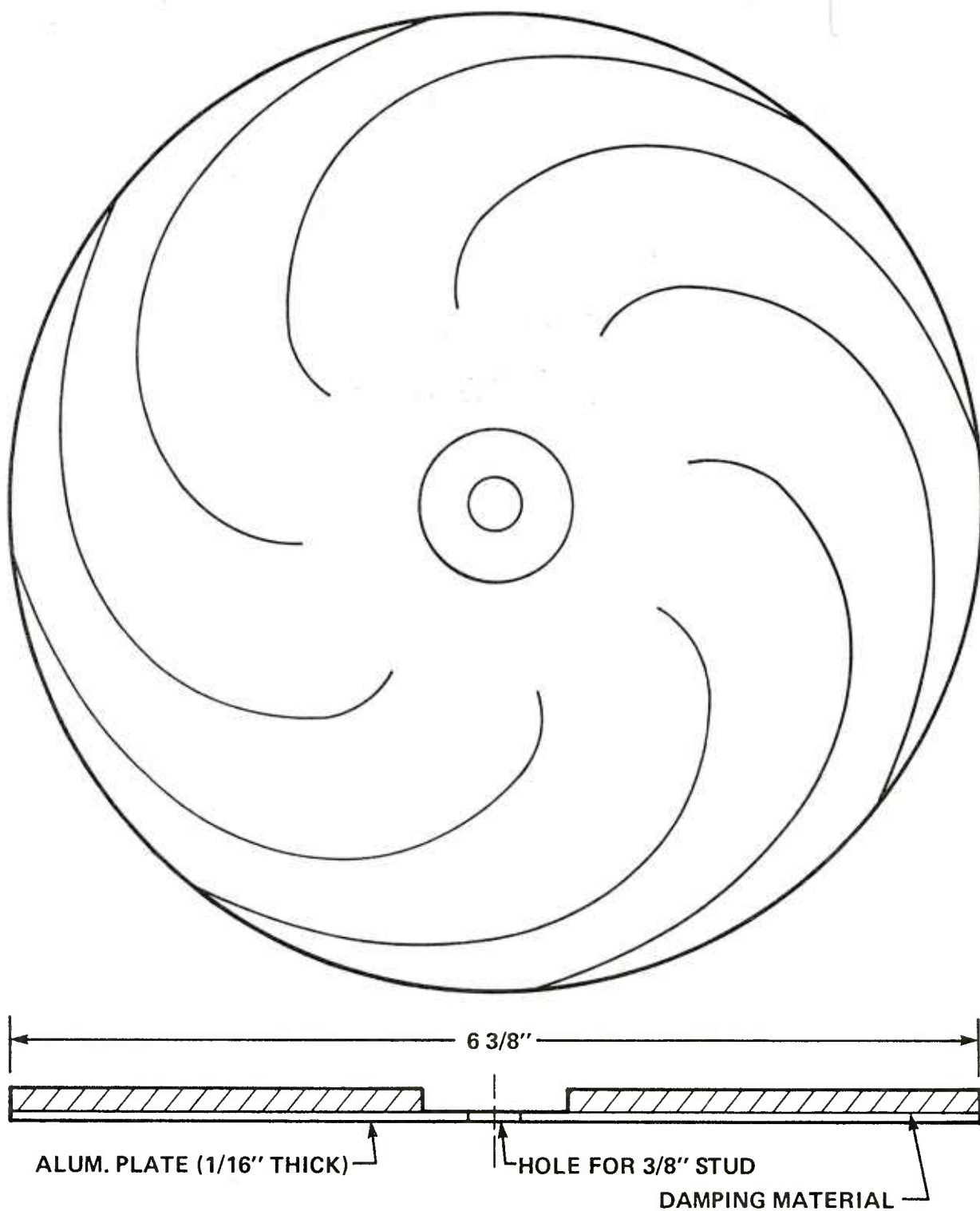
FIG. 7.   PATTERN FOR 8-SPIRAL DISK.
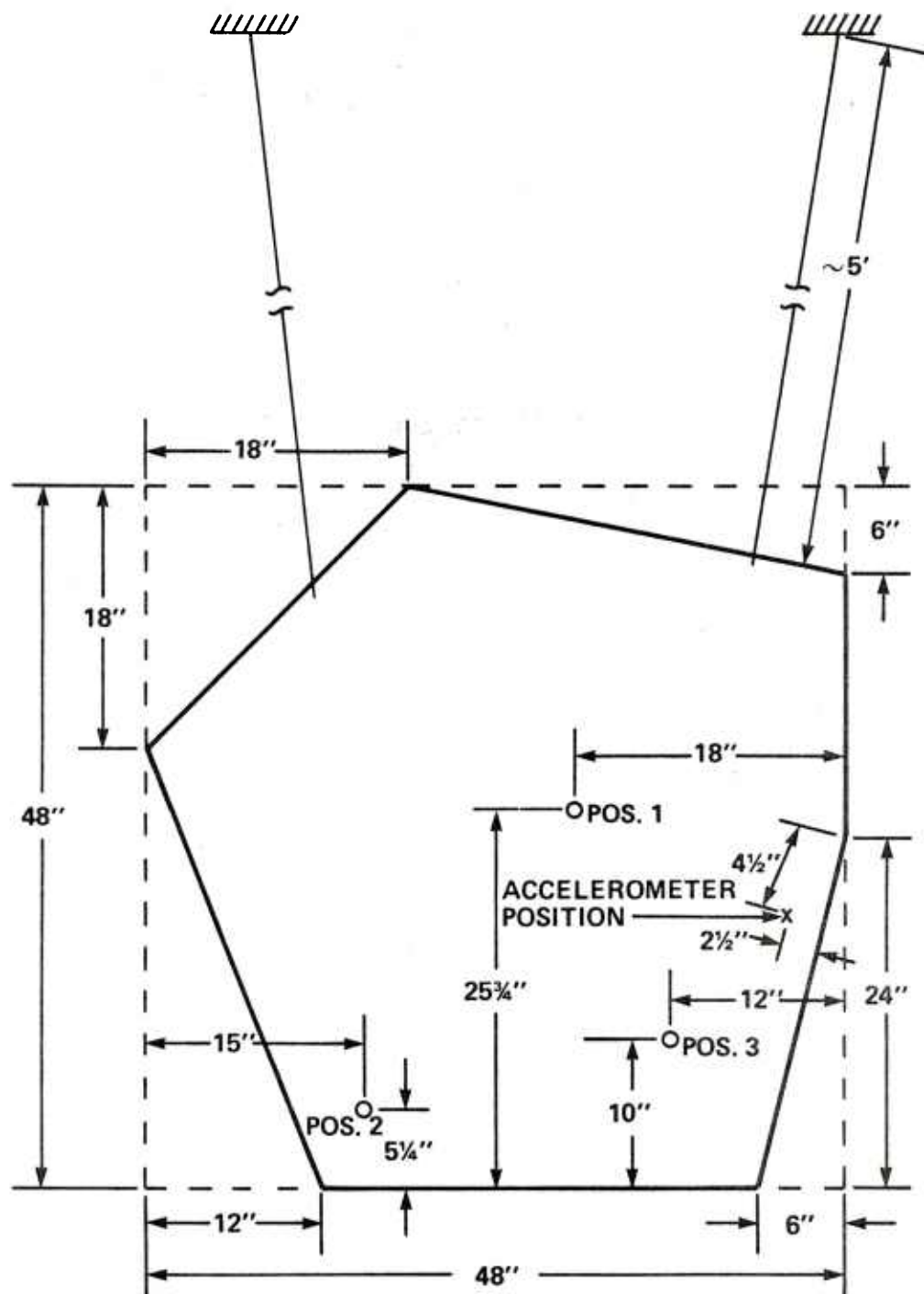
FIG. 8. EXPERIMENTAL PLATE STRUCTURE.
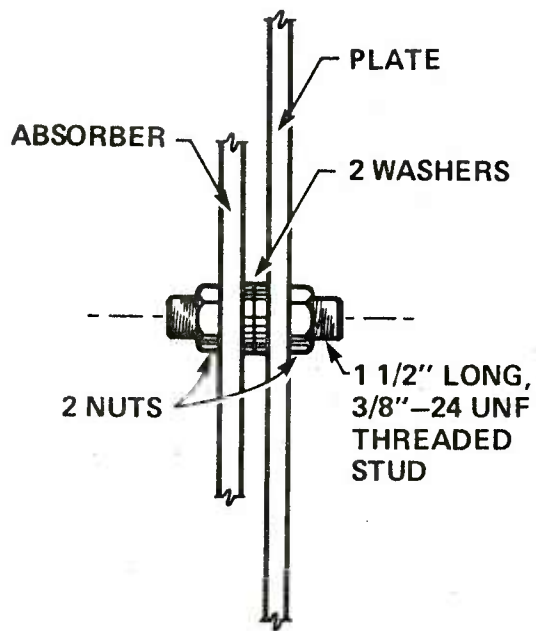
a. SINGLE ABSORBER BOLTED TO PLATE
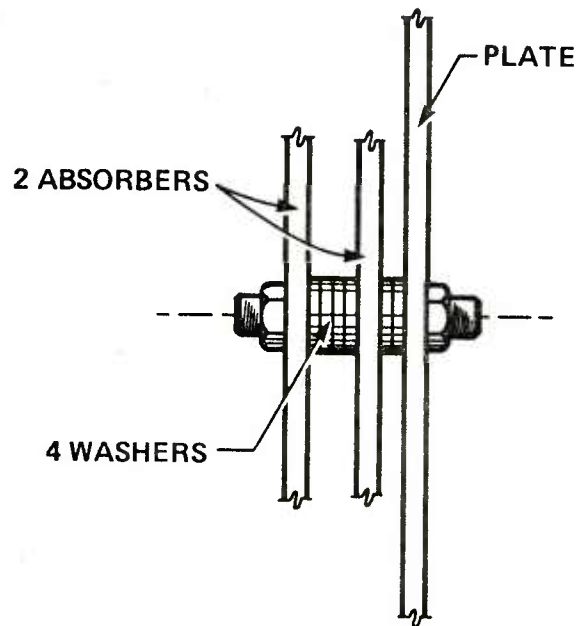
b. TWO ABSORBERS BOLTED TO PLATE
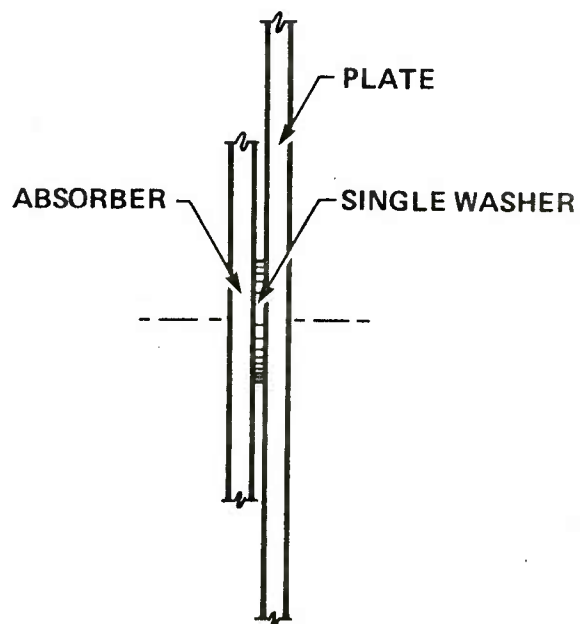
c. ABSORBER EPOXIED TO PLATE

FIG. 9. METHODS FOR ATTACHING ABSORBERS TO PLATE.
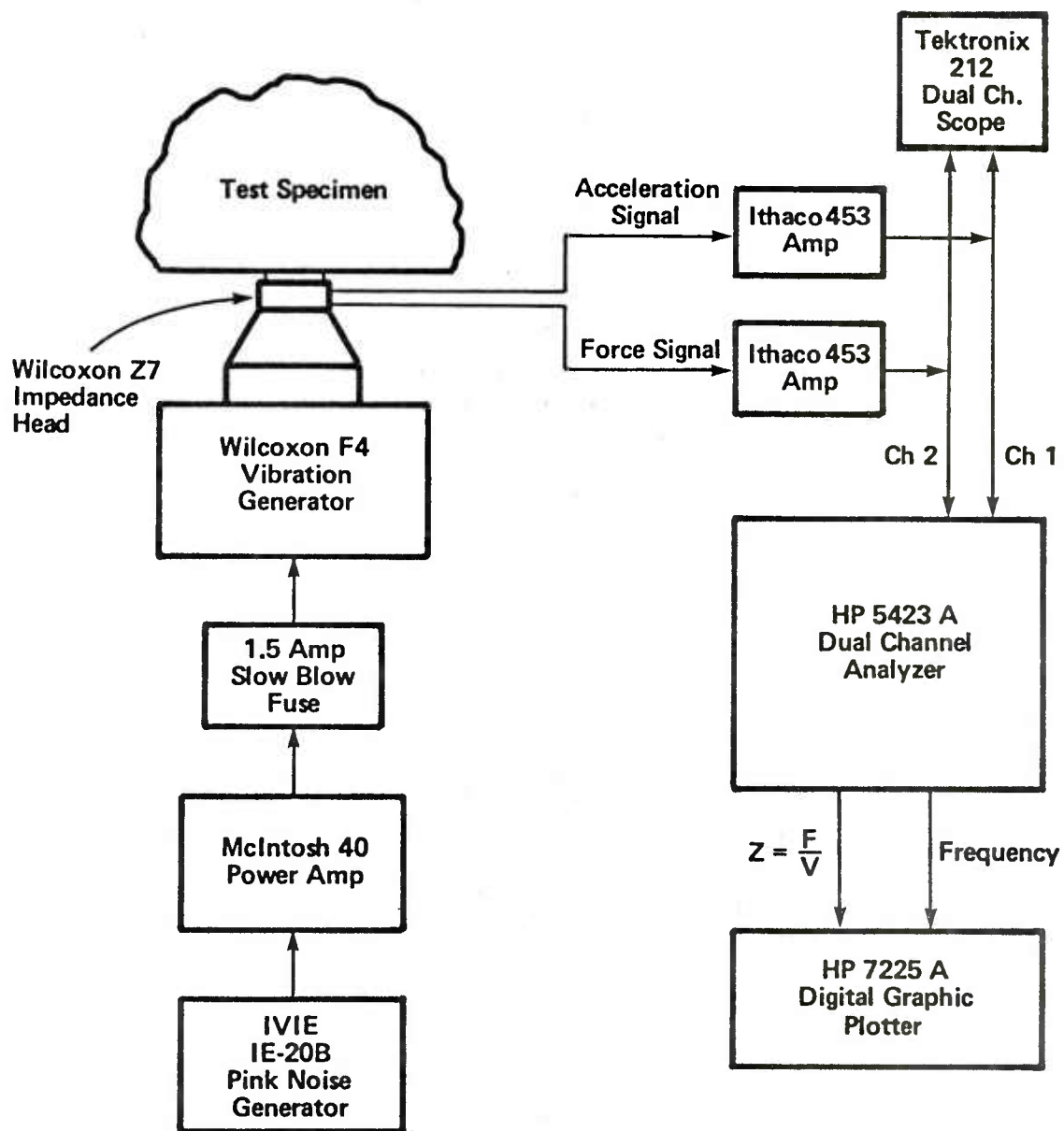
FIG. 10.   INSTRUMENTATION SYSTEM FOR MECHANICAL IMPEDANCE
          MEASUREMENTS.
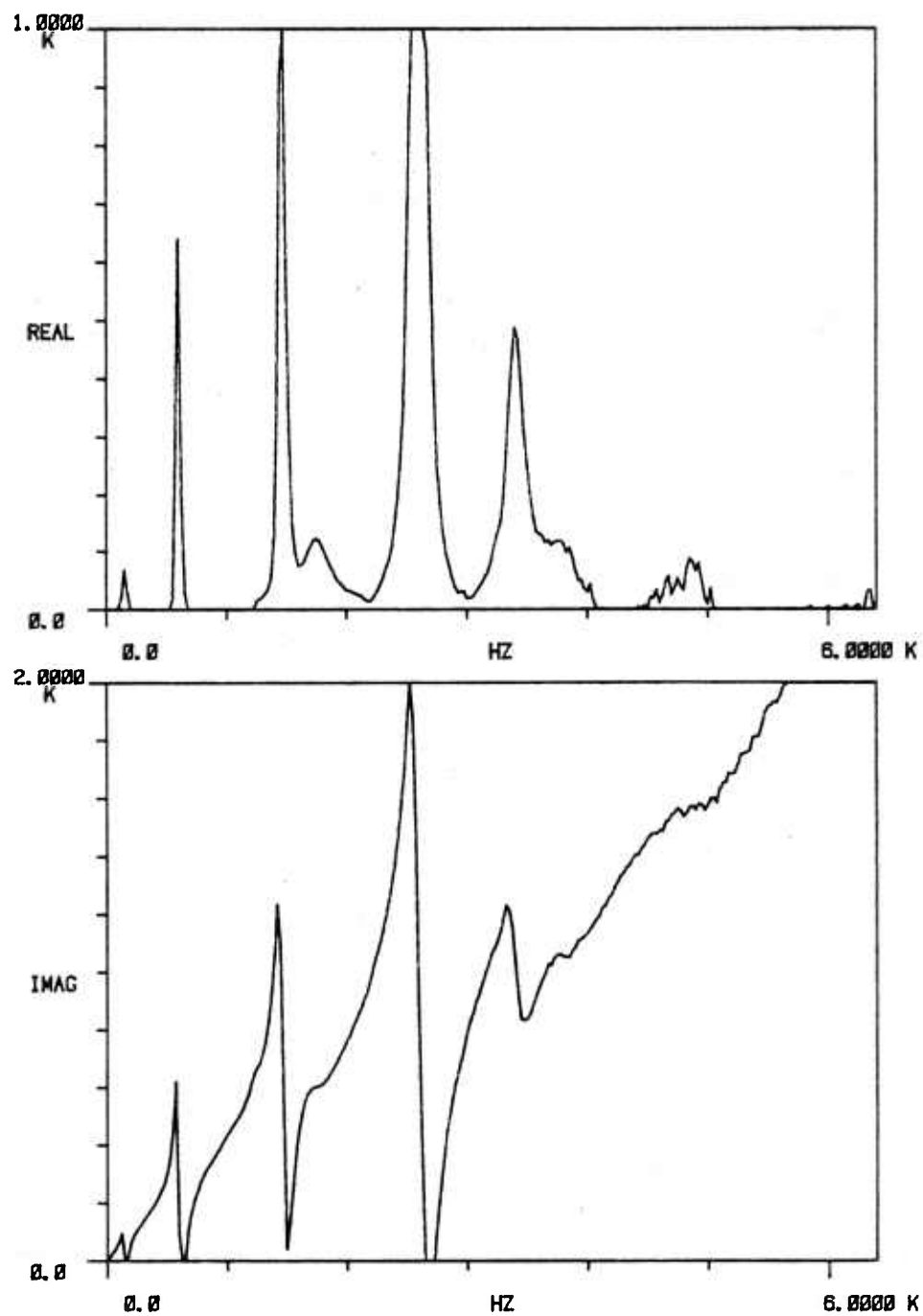
FIG. 11. IMPEDANCE OF TAPERED BEAM WITH ATTACHMENT HARDWARE.

38
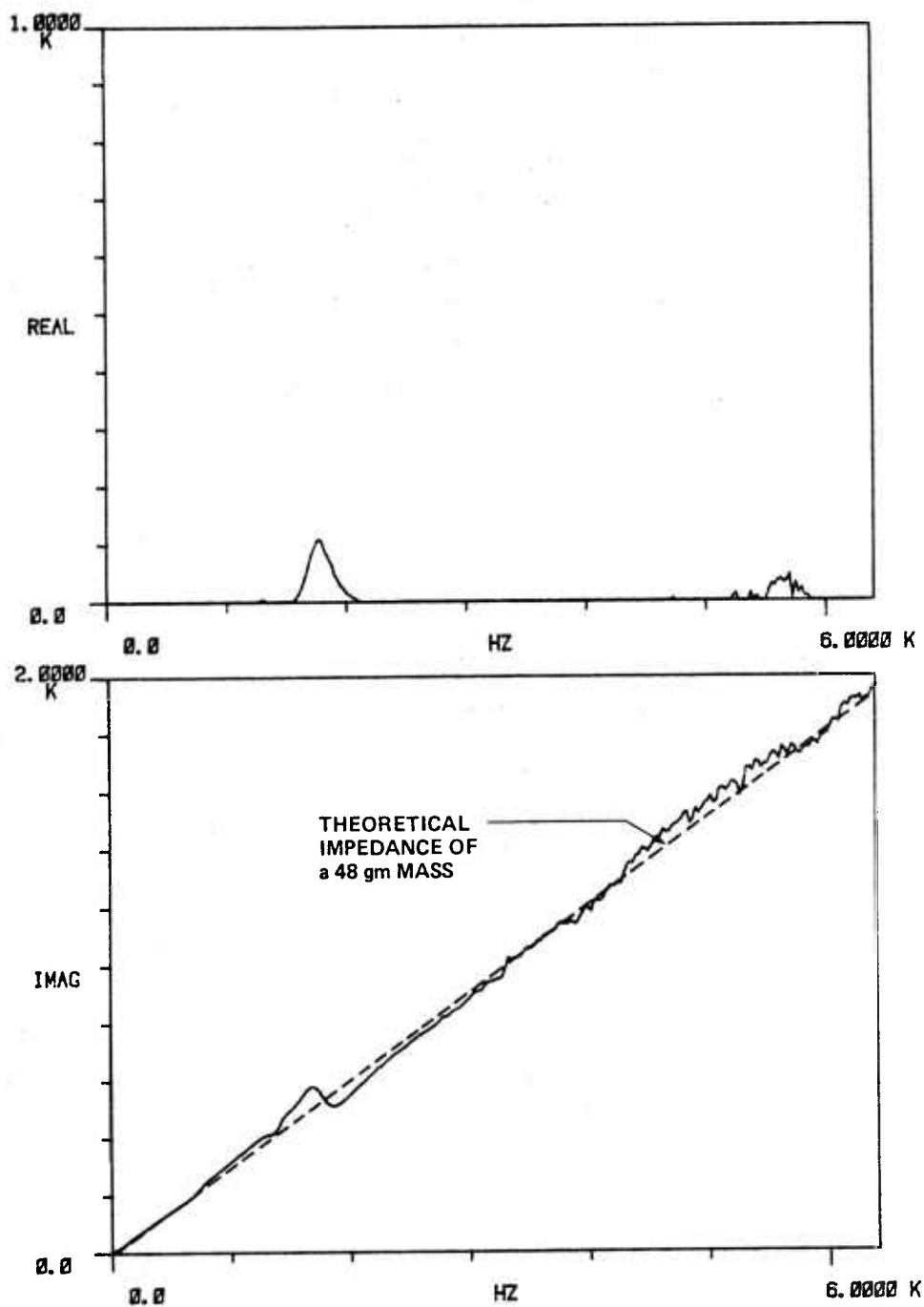
FIG. 12. IMPEDANCE OF ATTACHMENT HARDWARE FOR SINGLE ABSORBER.
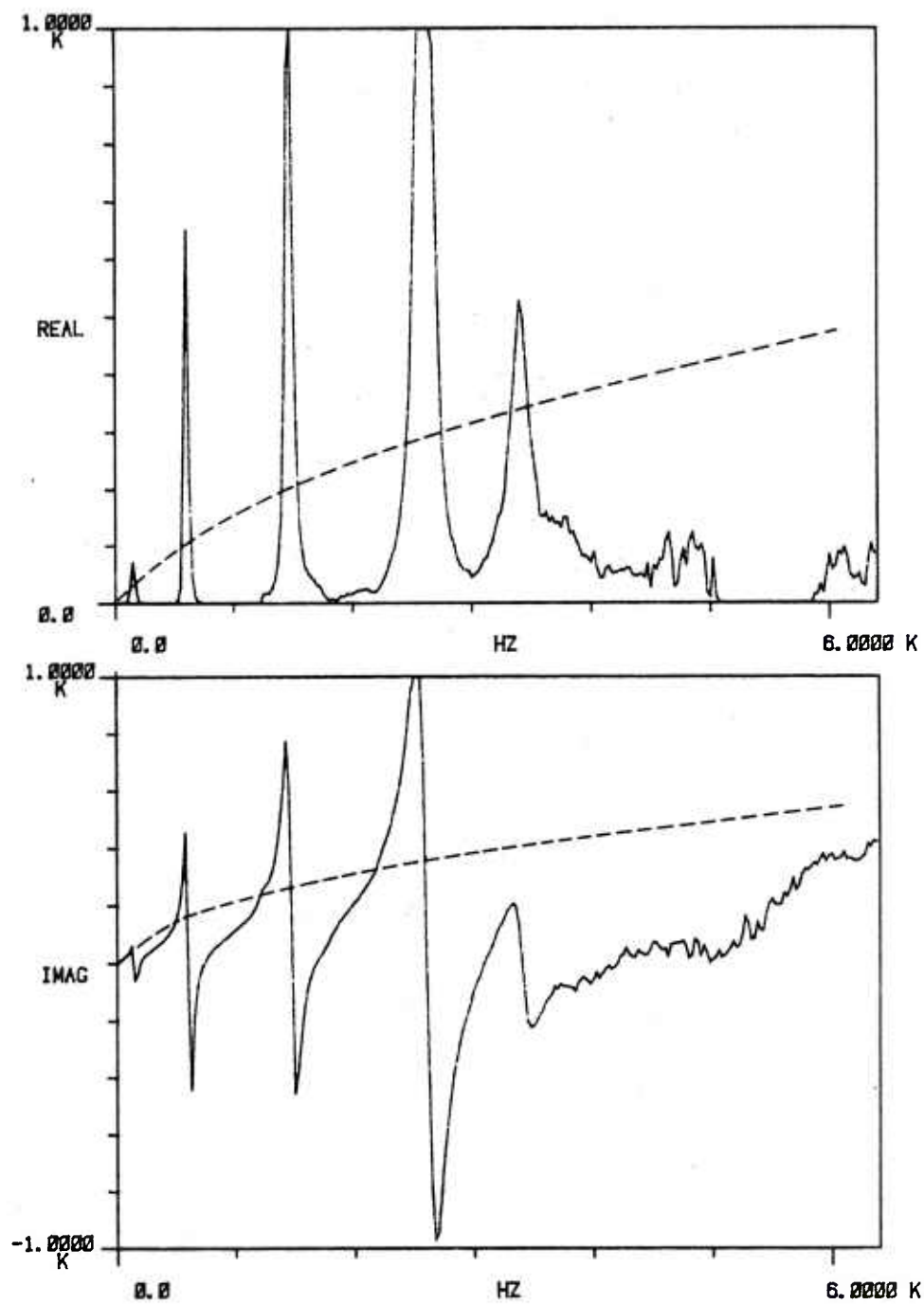
FIG. 13. IMPEDANCE OF TAPERED BEAM WITHOUT ATTACHMENT HARDWARE.

40
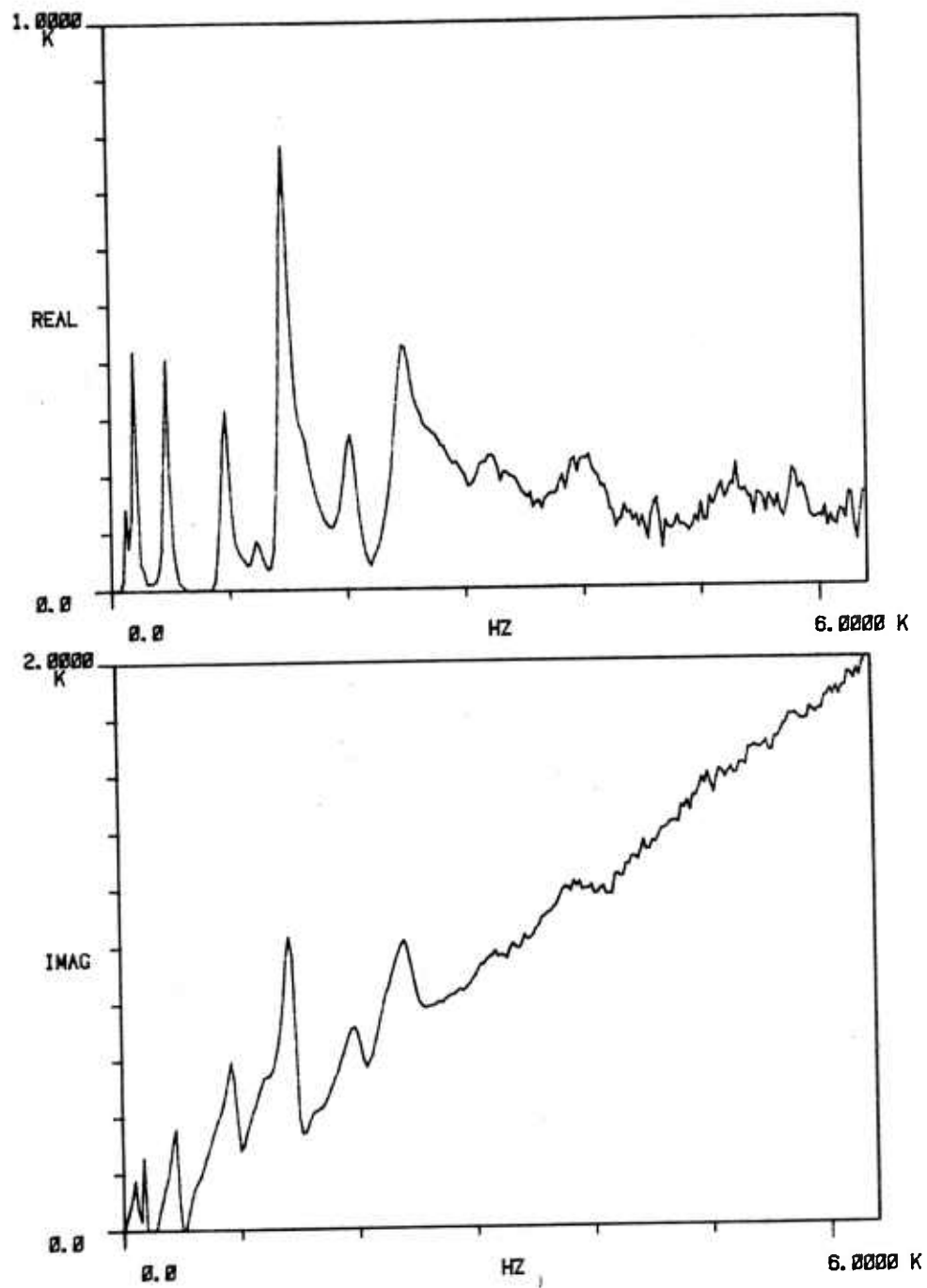
FIG. 14.   IMPEDANCE OF 8-SPIRAL DISK WITH ATTACHMENT HARDWARE.

41
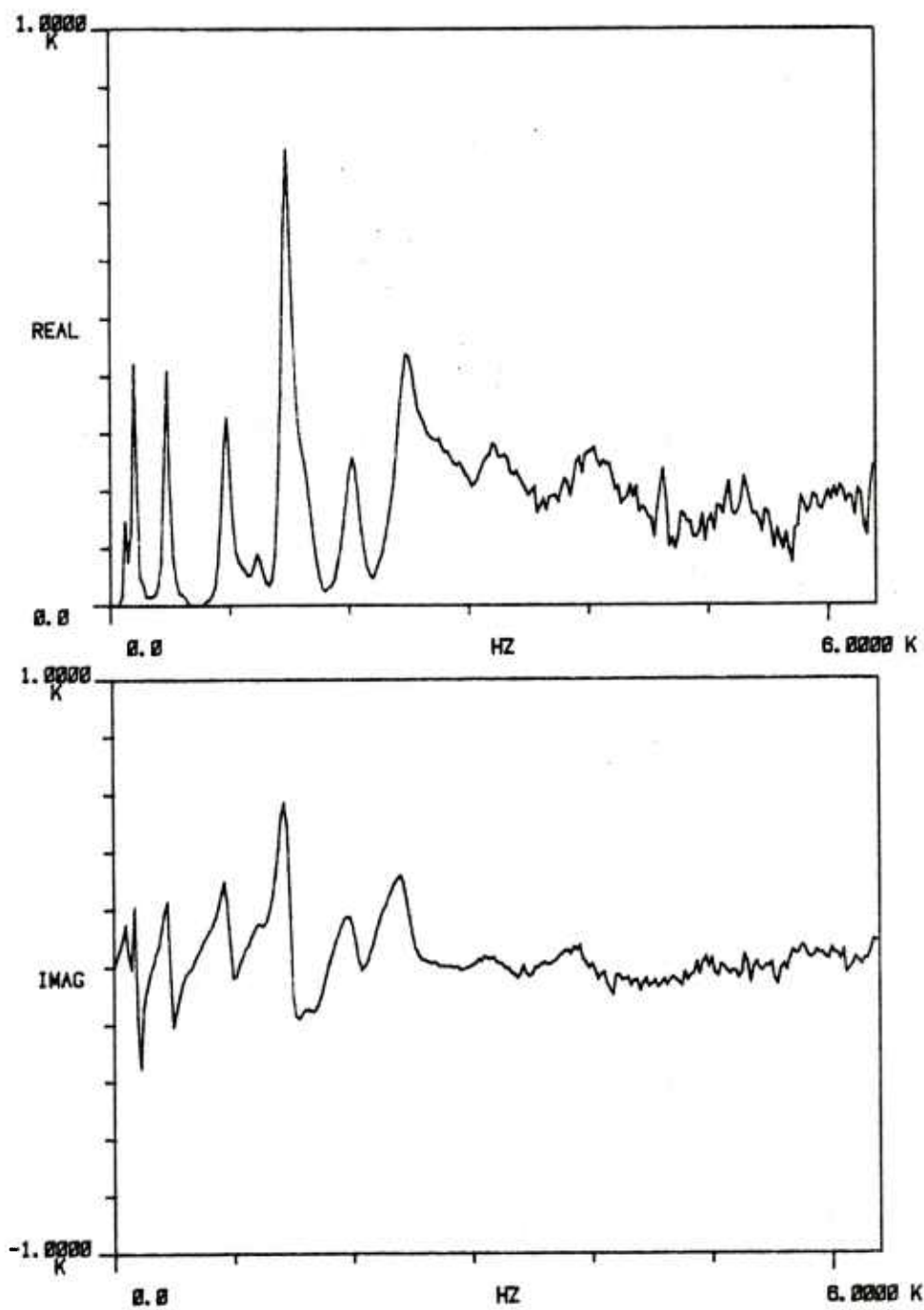
FIG. 15. IMPEDANCE OF 8-SPIRAL DISK WITHOUT ATTACHMENT HARDWARE.
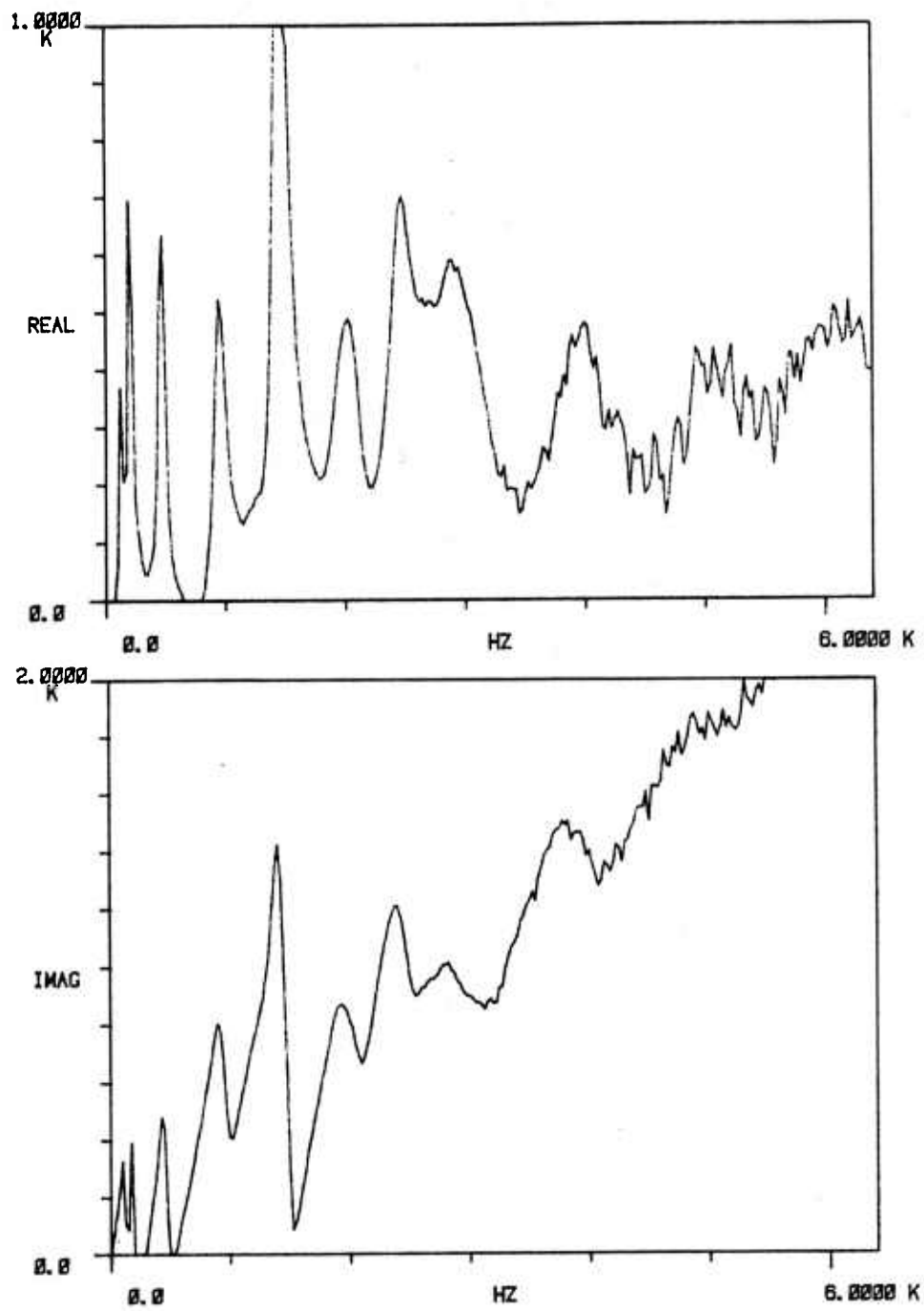
FIG. 16.   IMPEDANCE OF TWO 8-SPIRAL DISKS WITH ATTACHMENT
HARDWARE.

43
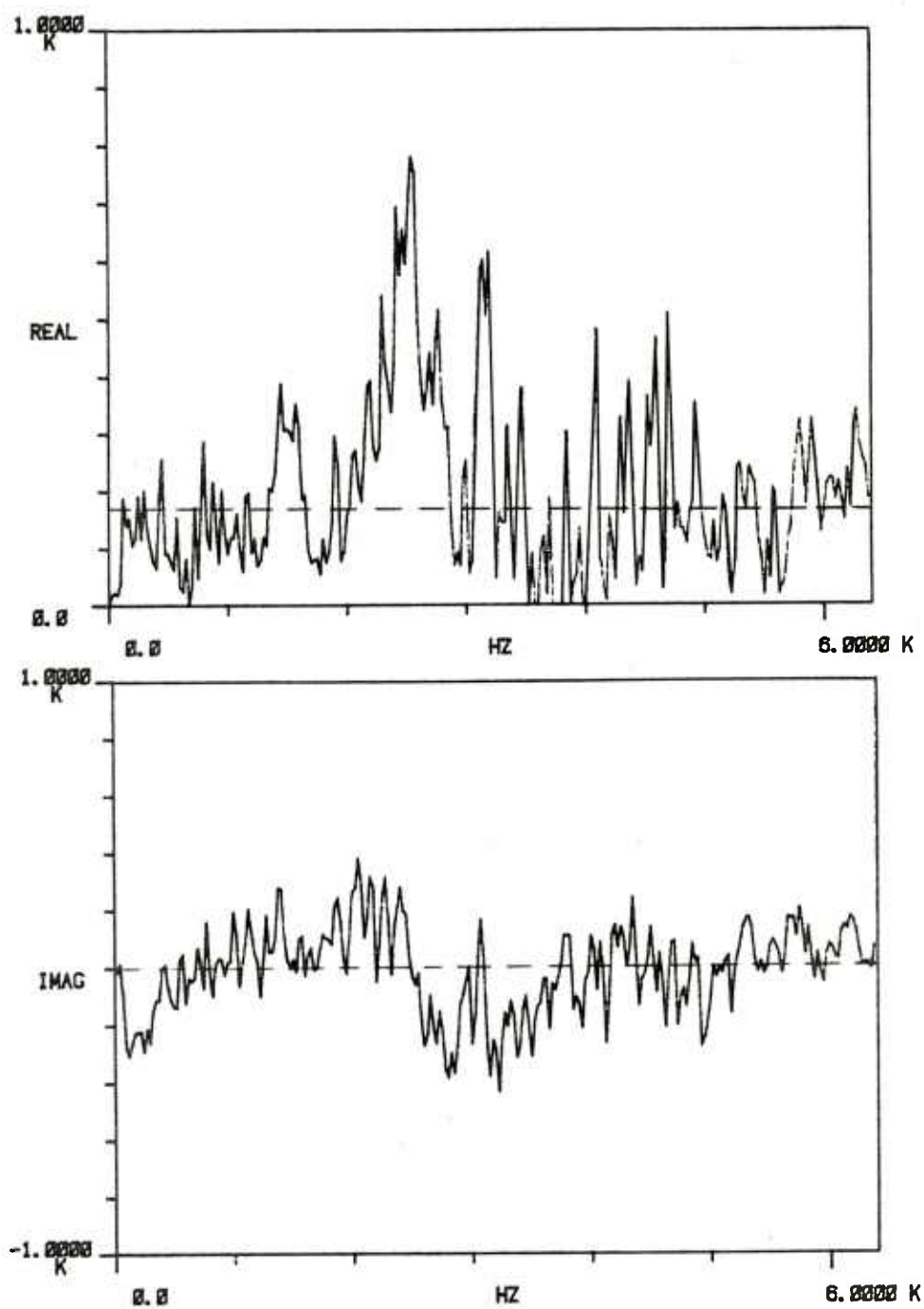
FIG. 17. IMPEDANCE OF EXPERIMENTAL PLATE WITHOUT ATTACHMENT
HARDWARE: ———— MEASURED AT POSITION 3; –––––
THEORETICAL FOR INFINITE PLATE.

44
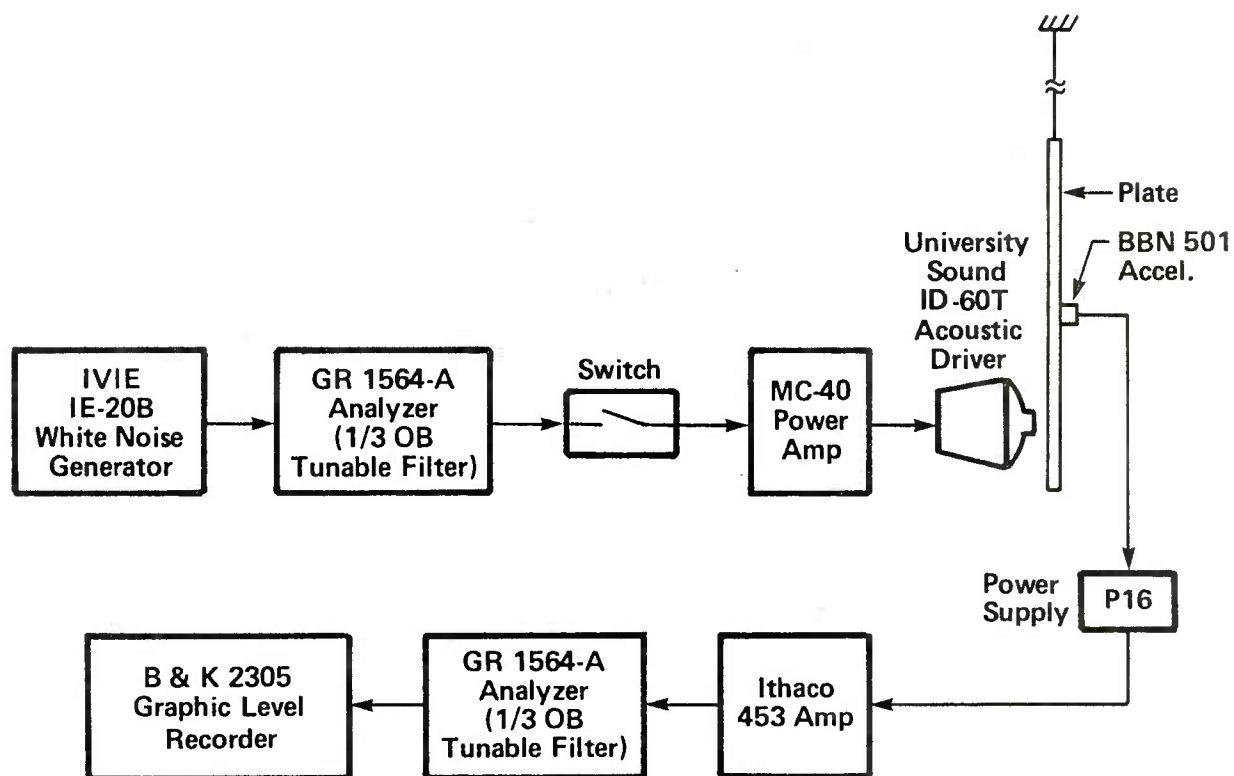
FIG. 18. INSTRUMENTATION SYSTEM FOR DECAY TIME MEASUREMENTS.

45
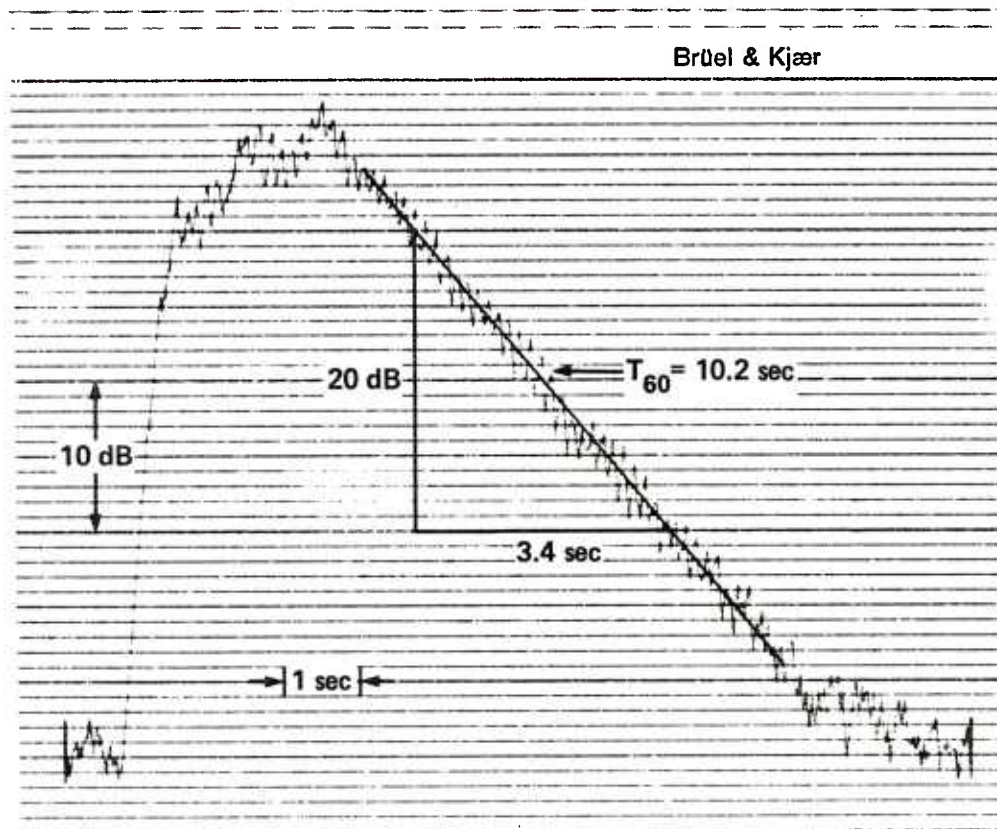
FIG. 19.   ACCELERATION LEVEL TIME HISTORY FOR UNDAMPED PLATE IN
THE 160 HZ 1/3 OCTAVE BAND.
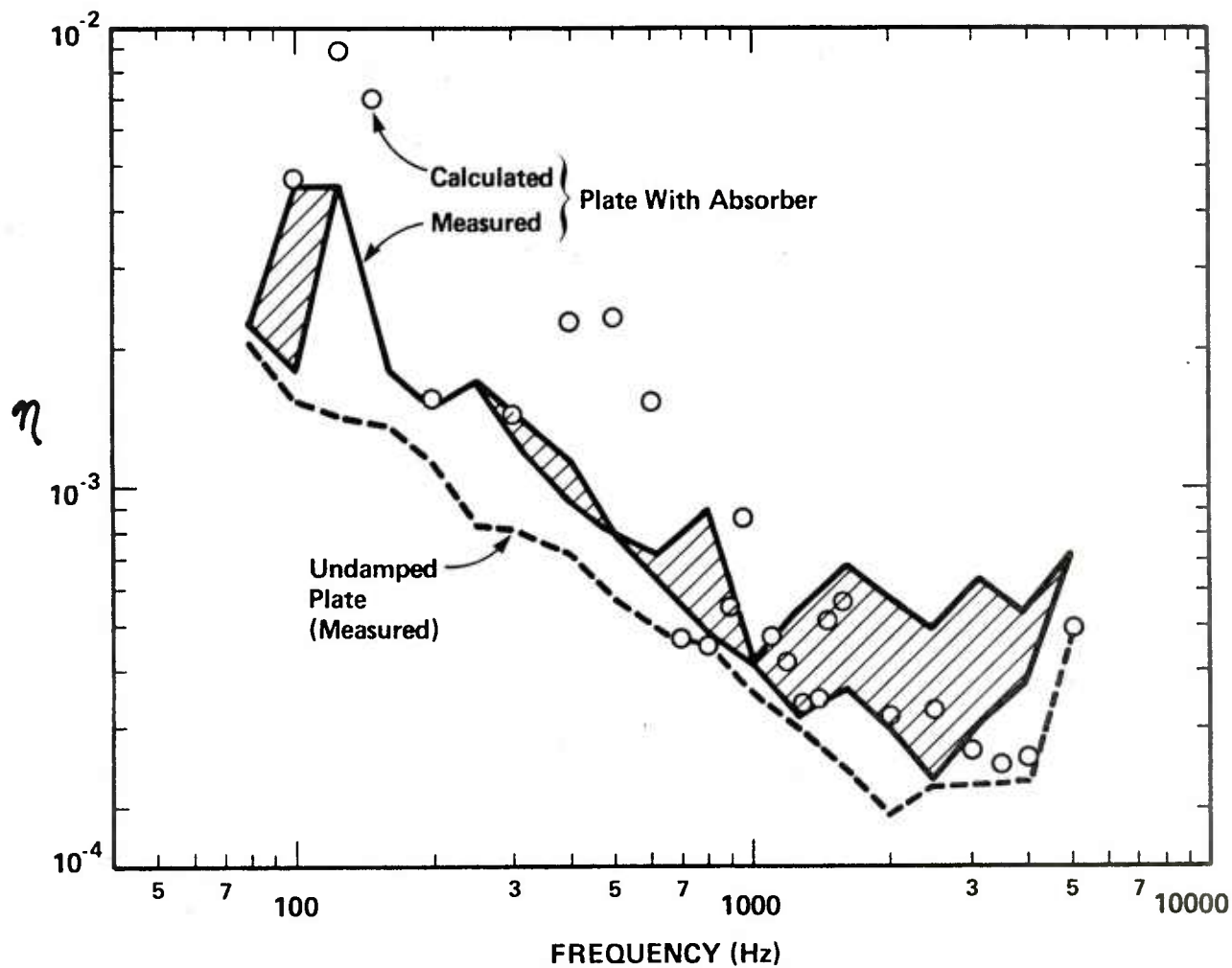
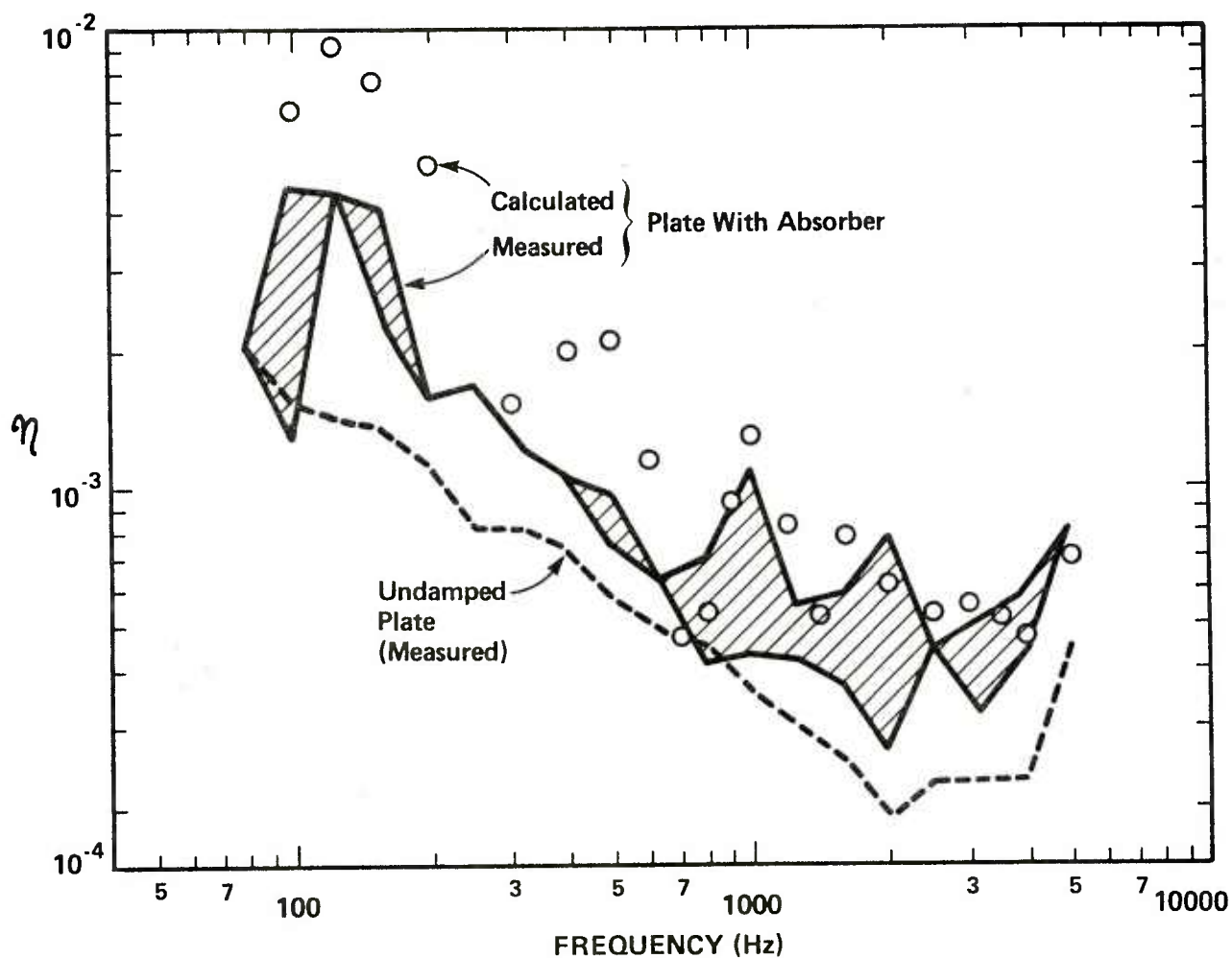FIG. 20. MEASURED AND PREDICTED LOSS FACTORS FOR PLATE WITH ONE
8-SPIRAL DISK ABSORBER BOLTED AT POSITION 3.

FIG. 21. MEASURED AND PREDICTED LOSS FACTORS FOR PLATE WITH ONE
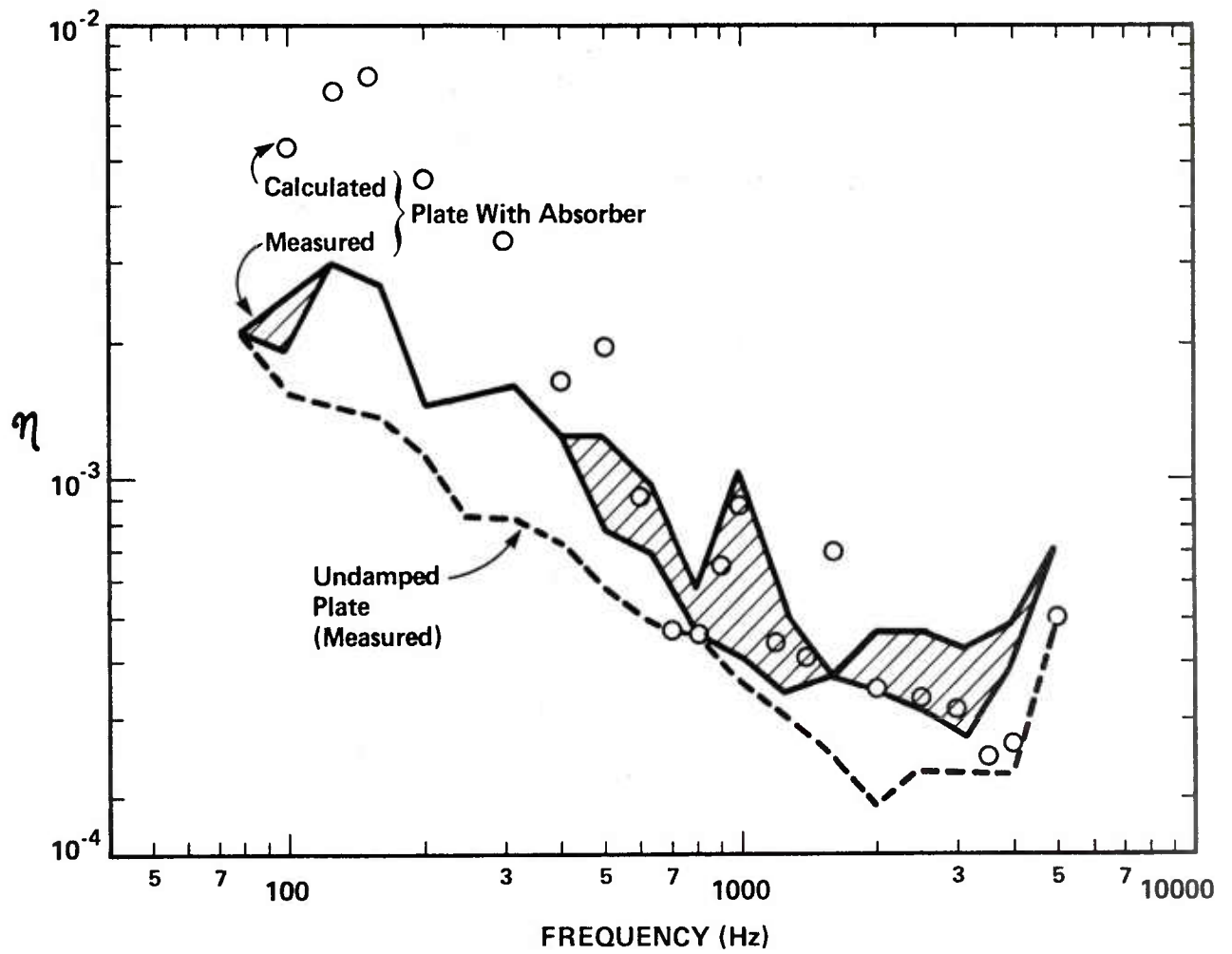8-SPIRAL ABSORBER EPOXIED AT POSITION 3.

FIG. 22.   MEASURED AND PREDICTED LOSS FACTORS FOR PLATE WITH TWO
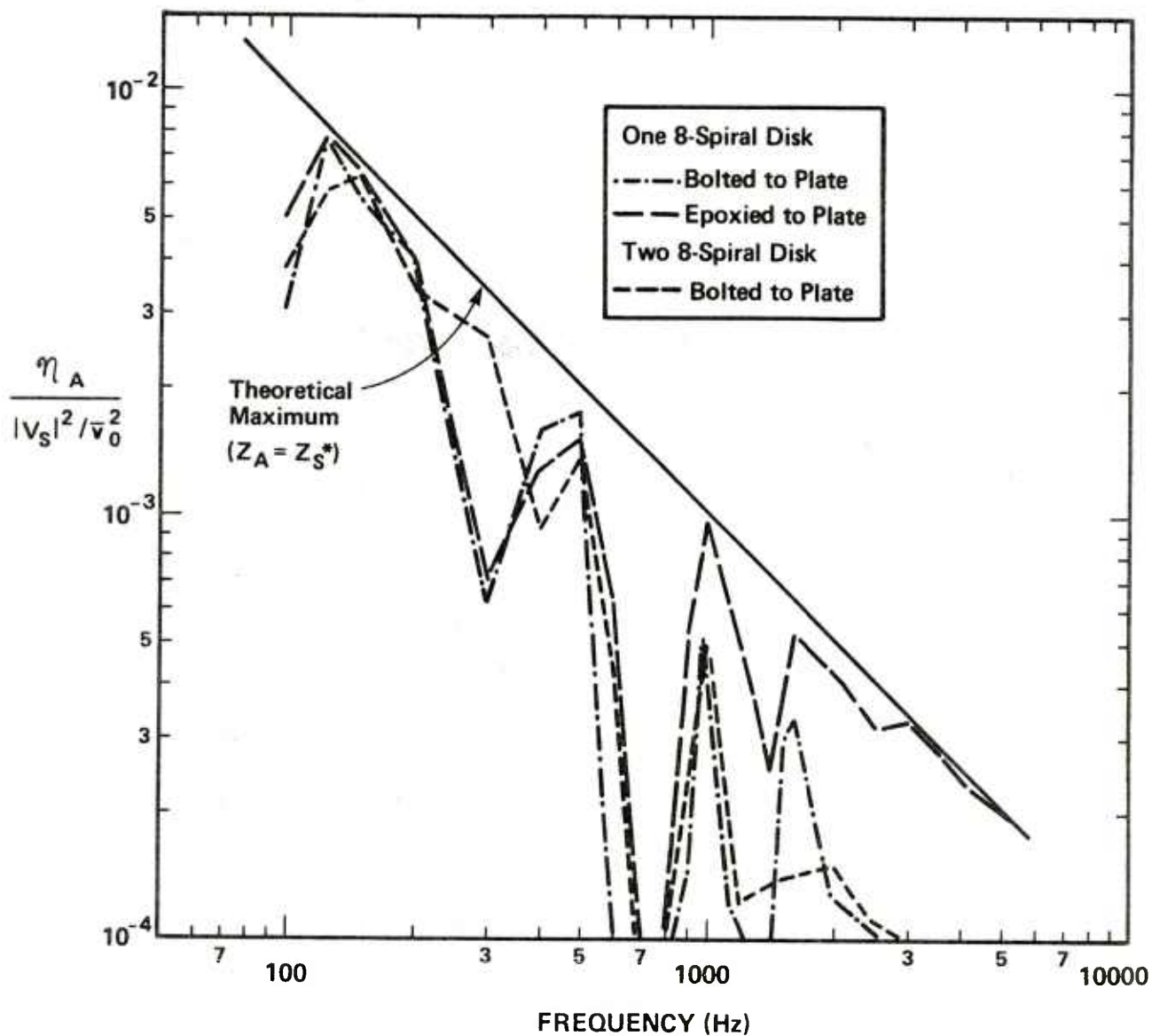   8-SPIRAL DISK ABSORBERS BOLTED AT POSITION 3.

49

FIG. 23. COMPARISON OF CALCULATED VALUES OF $\eta_A/(|V_s|^2/\bar{v}_0^2)$ FOR EXPERIMENTAL ABSORBERS WITH THE THEORETICAL MAXIMUM FOR AN ATTACHED ABSORBER.
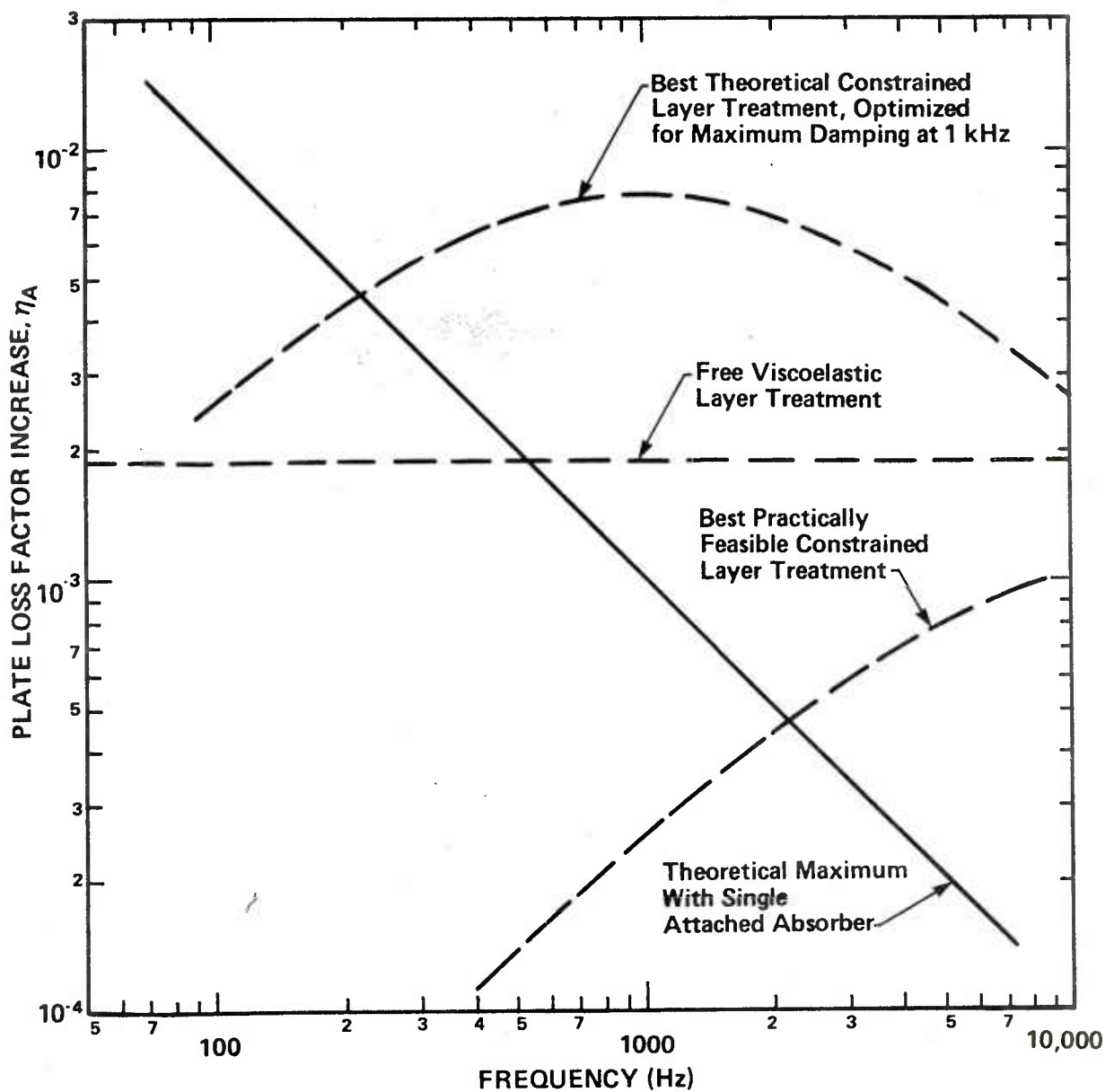
FIG. 24. COMPARISON OF LOSS FACTORS ACHIEVABLE IN THE EXPERI-
MENTAL PLATE BY MEANS OF DAMPING TREATMENTS WITH 2.6% OF
PLATE WEIGHT.

51